HYDROXIDE FORMATION AND CARBON SPECIES DISTRIBUTIONS DURING HIGH-TEMPERATURE KRAFT BLACK LIQUOR GASIFICATION

A Thesis
Presented to
The Academic Faculty

By

Michael Dance

In Partial Fulfillment
Of the Requirements for the Degree
Master of Science in the
School of Chemical and Biomolecular Engineering

Georgia Institute of Technology
August 2005

HYDROXIDE FORMATION AND CARBON SPECIES DISTRIBUTIONS DURING HIGH-TEMPERATURE KRAFT BLACK LIQUOR GASIFICATION

Approved by:

Dr. William J. Frederick, Jr., Advisor
School of Chemical and Biomolecular Engineering
Georgia Institute of Technology

Dr. Kristiina Iisa
Institute of Paper Science and Technology
Georgia Institute of Technology

Dr. Xin-Sheng Chai
Institute of Paper Science and Technology
Georgia Institute of Technology

Dr. Jeff Empie
School of Chemical and Biomolecular Engineering
Georgia Institute of Technology

Date Approved:
July 12, 2005

TABLE OF CONTENTS

LIST OF TABLES

LIST OF FIGURES

ACKNOWLEDGEMENTS

First and foremost, I would like to thank Dr. Frederick and Dr. Iisa for their guidance during this research project. Without their help in defining project objectives, guiding research techniques, and providing invaluable technical expertise, the work in this thesis would never have been completed. Also, I acknowledge Xiaoyan Zeng for all of her help with operating the LEFR and ensuring that the experimental runs were done correctly, and I also acknowledge Dr. Xin-Sheng Chai for all of his contributions to the experimental techniques and Headspace-GC data acquisition. I am grateful to the members of the Chemical Analysis Group at the Institute of Paper Science and Technology and Mike Buchanan for contributing the ionic species and total carbon analyses, and I am grateful to the research group of Larry Baxter at Brigham Young University for providing the black liquor used in this work. Additionally, I acknowledge Alan Ball and Chris Young for their assistance in operating the spray dryer, without which the black liquor solids would not have been adequately prepared for this work.

Of course, I am also grateful to friends, classmates, and family for all of their support over the years.

SUMMARY

This work focuses on high-temperature kraft black liquor gasification in the presence of H_2O and CO_2 in a laboratory-scale Laminar Entrained-Flow Reactor (LEFR). The effects of gasification conditions on hydroxide formation, carbon gasification rate, carbonate carbon and fixed carbon levels, alkali metal and sulfur species retention, and char yield were studied at atmospheric pressure and at 900-1000^{o}C, and at residence times of 0.5-1.5 s.

The results suggest that carbon gasification rates may be enhanced in the presence of H_2O and CO_2, with fixed carbon conversions of up to 95% at the earliest residence times at 1000^{o}C. CO_2 and H_2O gasifying agents cause a significant increase in carbonate formation, with 22% of the initial carbon input as carbonate compared to 16% with one gasifying agent. Carbonate levels increase to a high level and then decrease at 900^{o}C, but at 1000^{o}C, carbonate decomposition processes are more dominant and cause lower levels of carbonate even at early residence times. The results show that alkali metal retention is high until vaporization occurs after 1.4 s at 900^{o}C and at early residence times at 1000^{o}C. Moreover, the results show that sulfur retention is an exothermic process, as sulfur capture increases with temperature.

At 900^{o}C, no hydroxide is produced until after 1.4 s, but at 1000^{o}C, hydroxide appears to form readily even at the earliest residence times studied. The char produces a maximum mole percent of 18-19% hydroxide, starting at intermediate residence times at 1000^{o}C. Generally, hydroxide is not produced until fixed carbon conversions approach 95%. The results can be explained in terms of the interactions of phenolate and carboxylate catalytic species in the char product. The hydroxide

formation results suggest that it may be possible to develop a gasification-causticization process that does not require external chemicals and would make the energy-efficient and environmentally friendly black liquor gasification technology an economic reality.

CHAPTER 1

INTRODUCTION

1.1. Background

The United States annually imports 11 barrels of foreign oil for every 10 barrels produced domestically for all energy needs [37]. A major objective of the current National Energy Policy is to reduce dependence on foreign oil by increasing domestic energy supplies and using a more diverse mixture of domestic energy resources. According to the Department of Energy, renewable energy technologies, particularly those utilizing biomass, are capable of increasing domestic energy supplies by offering bioenergy and biobased products. If produced on a large scale, these products could simultaneously diversify domestic energy resources and improve energy independence. Overall, by efficiently using renewable energy, the United States will be able to utilize its domestic energy resources more efficiently and maintain economic prosperity. Moreover, the use of renewable energy could dramatically improve the environment for future generations.

1.2. Renewable Energy in the Pulp and Paper Industry

The pulp and paper industry is currently one of the largest producers and consumers of renewable energy in the United States. Renewable sources of energy come from cellulosic feedstocks used at pulp and paper mills, which originate from sustainably grown trees. The renewable sources of energy used at pulp and paper mills consist of biomass residual sources, such as wood wastes and bark, and black liquor, the biomass waste by-product of the pulping process. The total biomass energy

sources consumed at pulp and paper mills were an estimated 1.6 quads (1 quad = 10^{15} BTU) in 2002, and in 2001, all American primary sources of energy consumed 97 quads, with approximately 3% coming from biomass sources [37].

Pulp and paper mills already have the existing infrastructure to transport, store, and process biomass residual materials. In utilizing this existing infrastructure, the pulp and paper industry, with the aid of government funding, has explored new ways to recover useful energy and process chemicals more efficiently [37-40]. Gasification of biomass, particularly black liquor, provides an opportunity to enhance energy and chemical recovery throughout the pulp and paper industry. Gasification technology is in line with the overall objectives of increasing the nation's domestic energy supplies, promoting energy efficiency and conservation, and improving the environment. If implemented and commercialized on a wide scale, gasification technology will replace current technology that was first used almost a century ago, and in the process, it could make a major contribution to achieving the objectives. Additionally, its economic benefits could potentially allow the American pulp and paper industry to remain globally competitive [4, 21, 37, 38].

Essentially, gasification technology converts solid fuels, such as biomass, by partial oxidation of carbonaceous material (i.e., hydrocarbons within the fuel) to a product gas known as "syngas," which is mainly a mixture of CO_2, CH_4, CO, H_2O, and H_2. After sufficient cleaning, the hot syngas may be burned in a gas-fired turbine to produce electric power with a coupled generator, and the gas from the turbine exhaust duct may then be passed through a heat exchanger to produce steam. A portion of the steam is then transferred to a steam turbine for generating more electric

power. The combination of gas and steam turbines for electric power generation is referred to as a combined cycle (CC) operation.

In addition to CC operation, gasification technology provides opportunities for pulp and paper mills to produce transportation fuels and chemicals, such as methanol and dimethyl ether, due to the catalytic conversion of syngas. Additionally, the syngas from gasification can also produce pure hydrogen gas, which after catalytic enrichment, can be used in fuel cells [2-3]. Overall, the infrastructure of pulp and paper mills for handling biomass residual materials, such as black liquor, allows for the conception of gasification-based "biorefineries" capable of producing not only pulp and paper products, but also clean, renewable energy, chemicals, and fuels:

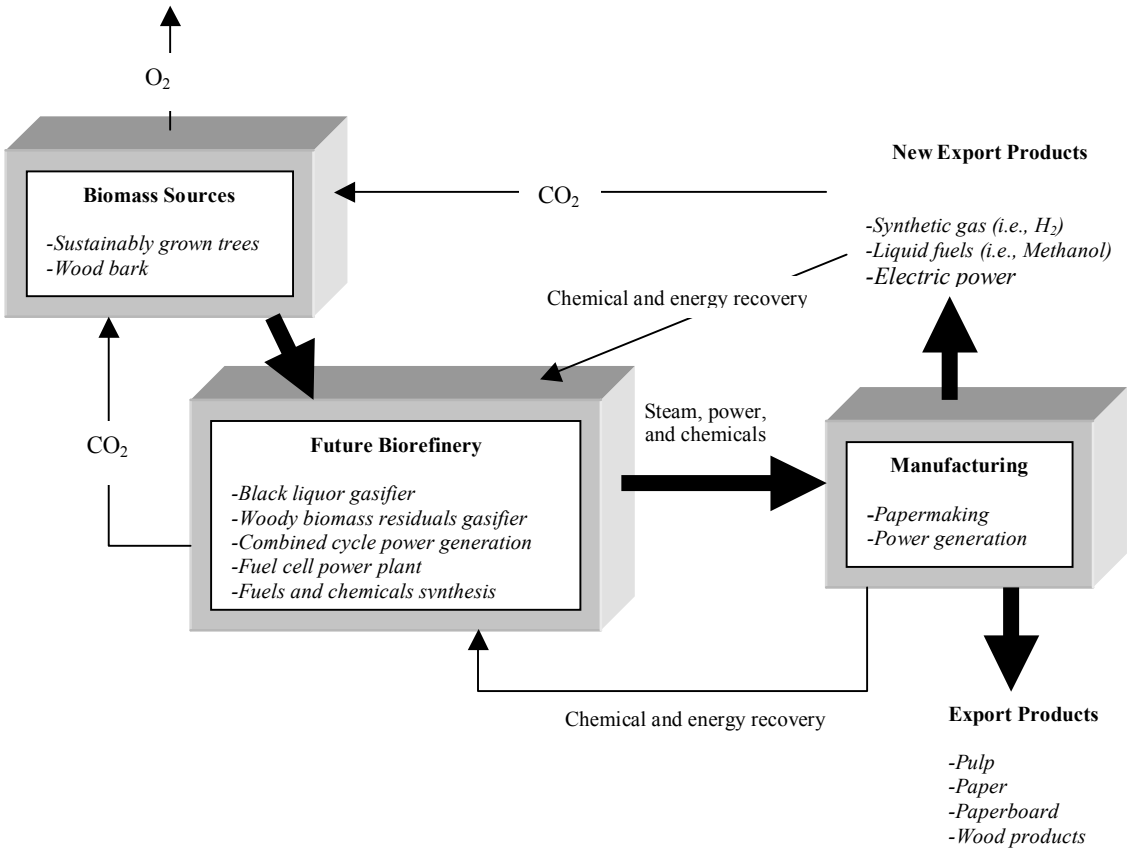

Figure 1.1: Future biorefinery operating at an existing pulp and paper mill [37]

The next few sections will elaborate on black liquor production and how the pulp and paper industry currently recovers process chemicals and useful energy from black liquor. The current technology will be compared to black liquor gasification, with particular emphasis on chemical recovery. Also, the environmental and societal impact of black liquor gasification will be discussed.

1.3. Papermaking and the Kraft Pulping Process

The papermaking process is one of the most energy-intensive processes in the world, and it is unique in that most of the energy consumed is generated from renewable biomass sources, such as black liquor [21, 37-40]. Black liquor is a biomass waste by-product produced during the pulping portion of the papermaking

process, whereby wood from trees is converted to cellulosic fibers for paper. It is an important renewable energy source in the pulp and paper industry, and it is currently an underutilized fuel source in the United States, as well as other paper-producing regions of the world. Approximately 240 million tons of black liquor is produced and burned annually, and its fuel energy value is equivalent to 460 million barrels of crude oil per year [21]. In contrast, 3.8 billion tons of oil and 1 billion tons of gasoline are produced and burned annually. According to Reeve, black liquor is currently the sixth most important fuel in the world:

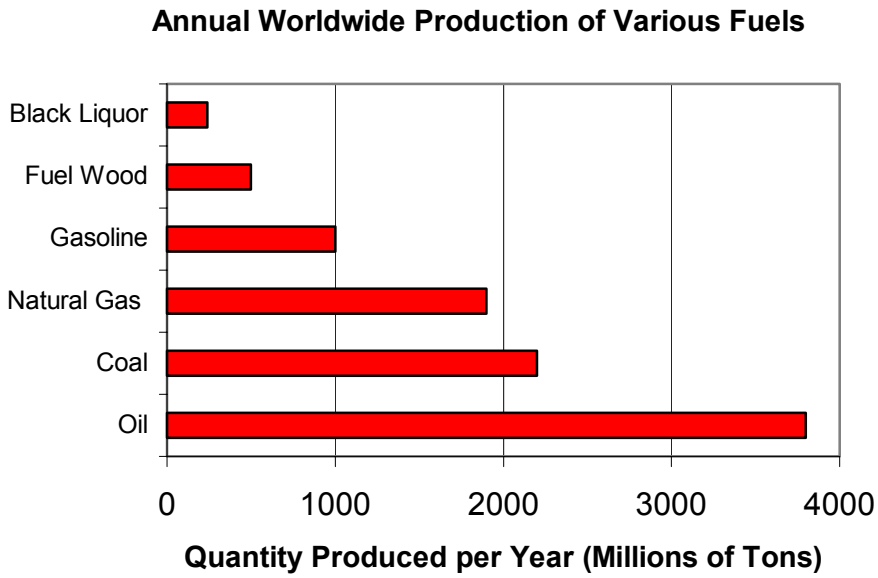

Figure 1.2: Annual production rates of primary fuels [57]

Essentially, the papermaking process converts fibrous raw materials into pulp, paper, and paperboard. The main sections of the process consist of wood pulping, chemical and energy recovery, pulp drying, bleaching, and papermaking, with pulping, drying, and chemical and energy recovery being the most energy-intensive

sections [47]. While there are several methods for pulping wood, the most common method in the United States is the so-called "kraft" process. The kraft process is preferred due to its relatively rapid pulping rates, its ability to produce a strong pulp, its adaptability to many types of wood feedstocks, and its low chemical costs [6, 47, 62]. Figure 1.3 shows a simplified schematic diagram of the kraft pulping process and the corresponding chemical and energy recovery process:

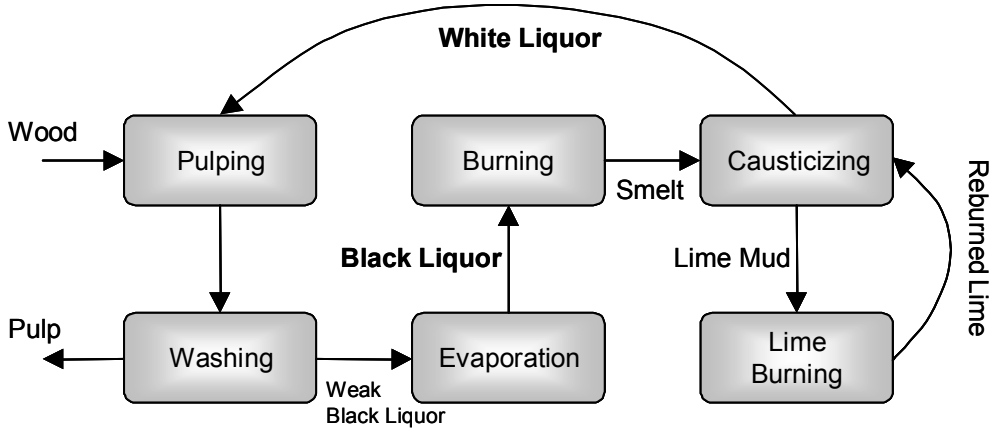

Figure 1.3: The kraft pulping process and chemical and energy recovery cycle [67]

The kraft pulping process involves chemical extraction of cellulose from wood. Wood is a natural composite material consisting of hollow, flexible tubes of cellulose fibers (long, straight chains of glucose molecules) that are bound together in a 3-dimensional matrix by lignin (a phenolic polymer network):

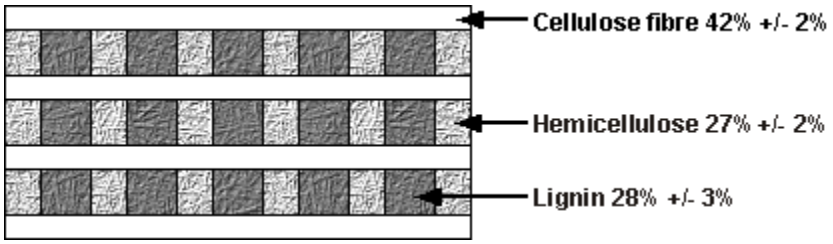

Figure 1.4: Structure of wood and average composition of wood components [7]

Wood also consists of hemicellulose, which is a water-soluble conglomerate of short-chained glucose and polysaccharide molecules, and toxic extractive chemicals, which account for 2-3% of softwoods [7]. Extractive chemicals, or extractives, consist of plant hormones, fatty acids, and resins, which help trees grow and resist disease.

At a conventional kraft pulp mill, logs of wood from sustainably grown trees are chipped and debarked, and the clean chips are transferred to digesters, or pulping vessels, for pulping. The wood chips are first pre-steamed to soften them and remove trapped air pockets, and then they are mixed in the digesters with a highly caustic, alkaline solution called white liquor, which consists mainly of NaOH and Na_2S. They are then pressurized and "cooked" at 160-170 ^{o}C. During cooking, the alkaline liquid permeates the chips and neutralizes the organic acids within the composite structure. After 2-4 hours of cooking, the cellulose fibers are extracted from the chips in the form of pulp slurry, while the lignin, hemicellulose, and extractives dissolve into the white liquor. The fibers that constitute the pulp slurry are washed and move onto the bleaching and papermaking processes, while a liquid waste by-product remains. This liquid waste is the black liquor, which consists of alkali lignin, hemicellulose, extractives, and spent pulping chemicals. Generally, only 40-55% of the wood becomes pulp in the kraft process, while the remainder becomes black liquor [47].

The black liquor typically has a solid content of about 14-17% by weight in a highly viscous liquid solution. To make it a useful fuel, the black liquor, known as weak black liquor at this point, is concentrated in a series of multiple-effect evaporators and direct-contact evaporators to a viscous liquid with a solids content of 65-80% by weight. Then, the concentrated black liquor is transferred to the chemical and energy recovery system. Overall, organic matter (mainly alkali lignin and hemicellulose-based hydroxy acids, with small amounts of extractives) represents about 60% of the black liquor, with the balance being inorganic matter derived from the pulping chemicals. The organic matter makes the black liquor solids suitable for being a low-grade fuel, with effective calorific values of approximately 12-13 MJ/kg, compared to 28 MJ/kg for coal, and 17 MJ/kg for wood [34].

1.4. Chemical and Energy Recovery in Kraft Pulp Mills: Current Technology

Typically, pulp mills burn black liquor in recovery boilers, whereby the liquor undergoes complete combustion with air to form a gaseous product, while leaving behind a molten slag called *smelt*. Figure 1.5 shows a simplified schematic of a conventional recovery boiler used at pulp mills:

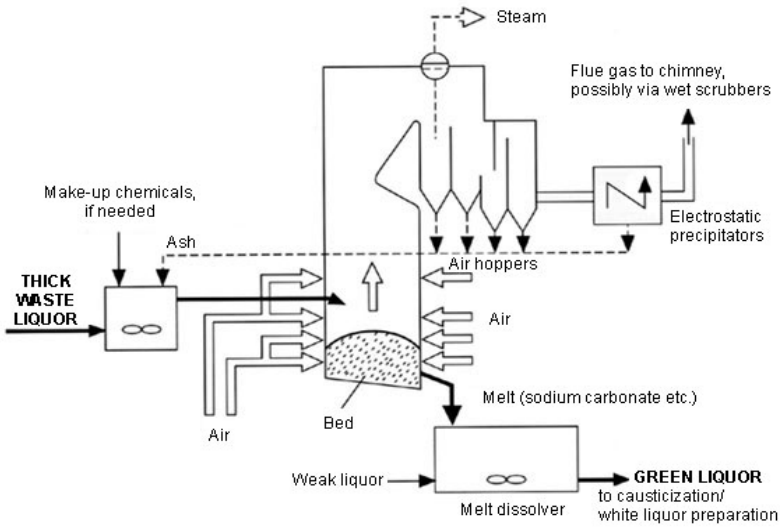

Figure 1.5: Conventional recovery boiler design [23]

The concentrated black liquor is initially sent to an atomizer to produce spherical droplets, and special spray nozzles spray these droplets into the furnace of the recovery boiler. Air is blown into the furnace at several levels of the boiler to react with the droplets for combustion. The droplets are dried and settle to the bottom of the recovery boiler to form a char bed, and during this process, the organic fraction of the black liquor is completely combusted via pyrolytic processes discussed in Chapter 2. The combustion processes occur at operating temperatures of 900-1100^{o}C and produce a hot flue gas, which passes through a matrix of steam tubes to produce high-pressure steam. These tubes are located in various parts of the boiler, such as within the walls or in an economizer. The hot flue gas contains H_2O, CO_2, CO, CH_4, H_2, light total reduced sulfur (TRS) gases (i.e., H_2S), SO_2, particulates, some alkali metal vapors, and condensable organic compounds called tars [30]. The flue gas is filtered and cleaned, with electrostatic precipitators removing particulates, before it is released into the atmosphere.

While the flue gas is cleaned, some of the high-pressure steam enters a steam turbine to generate electricity, while the rest of the steam is used as process steam. During liquor combustion, the alkali salts in black liquor are converted primarily to carbonate species, and inorganic sulfur species originally in the liquor are reduced to sulfide species. The solids that travel to the bottom of the recovery boiler are transformed into the smelt, which contains most of the inorganic matter and almost all of the sulfur species originally in black liquor. The liquid smelt, which contains mainly Na_2CO_3 and Na_2S (with small amounts of corresponding potassium compounds), leaves the recovery boiler and is dissolved in water. After being dissolved in water, the liquid smelt is referred to as *green liquor*.

In the final process of the chemical recovery system, the aqueous green liquor is converted to re-generated white liquor, which is then recycled back to the digesters for pulping. The common procedure is referred to as the *lime cycle*, which is shown in Figure 1.6:

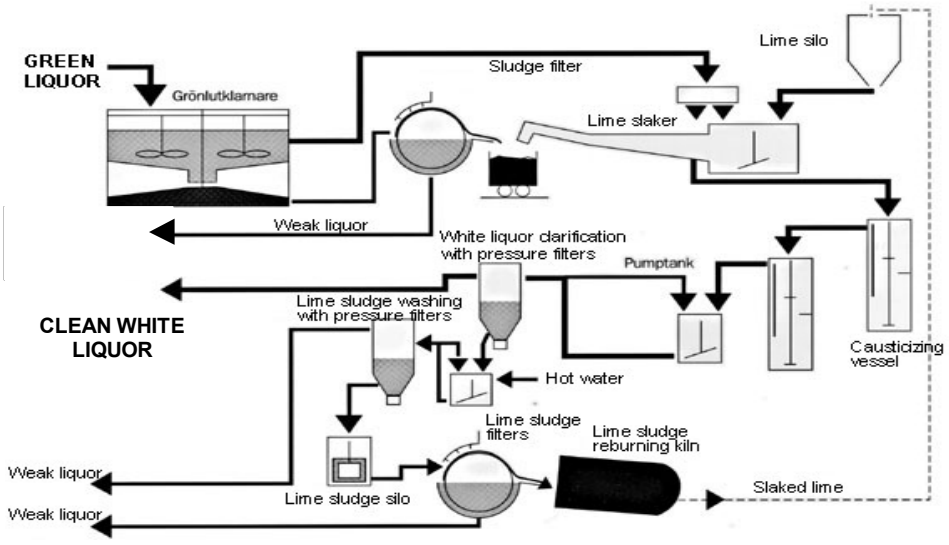

Figure 1.6: White liquor preparation via lime cycle [23]

Sludge is removed from the green liquor by clarifiers, and then the green liquor is sent to a lime slaker, where it reacts with lime (CaO produced from the thermal degradation of $CaCO_3$ in a lime kiln). The water in the green liquor reacts with or "slakes" the CaO to produce $Ca(OH)_2$, which is transferred to causticization vessels with the liquor. During causticization, the Na_2CO_3 in the green liquor reacts with $Ca(OH)_2$ to form NaOH and $CaCO_3$. From there, the $CaCO_3$ is separated from the resultant substance (lime mud) in clarifiers, thus producing white liquor. The white liquor is recycled back to the digesters for pulping, while the $CaCO_3$ is recycled to the lime kiln, where it is burned to re-generate CaO. The lime kiln is an energy-intensive process, and it requires the burning of significant amounts of fuel oil or natural gas to generate the needed energy [37].

The black liquor combustion reactions create a highly corrosive environment within the recovery boiler. The use of water as a heat transfer medium within the recovery boiler creates the potential for smelt-water explosions, which occurs when water leaks from the boiler tubes into the smelt at the bottom of the boiler. Although pulp mills have used conventional recovery boilers for almost a century, there are many problems and disadvantages associated with them: (1) low electrical and thermal efficiency, (2) releases of total reduced sulfur (TRS) gases resulting in odor problems, and SO_2 releases that contribute to acid rain, (3) large CO_2 and wastewater discharges, (4) the possibility of dangerous smelt-water explosions, and (5) the high costs of capital, operation, and maintenance [62].

1.5. Black Liquor Gasification: New Opportunities for Chemical Recovery

The kraft recovery process has utilized recovery boilers for almost a century, with modern recovery boilers being used as early as the 1930's. While the designs have become more sophisticated since then, the problems associated with recovery boilers have caused the pulp and paper industry to consider alternative chemical recovery technologies. The gasification of black liquor and woody biomass residual materials is being developed in earnest as an alternative to the current technologies. Gasification may become part of integrated gasification and combined cycle (IGCC) operation, or lead to pulp mills becoming biorefineries [37]. Figure 1.7 shows a simplified schematic for the black liquor IGCC:

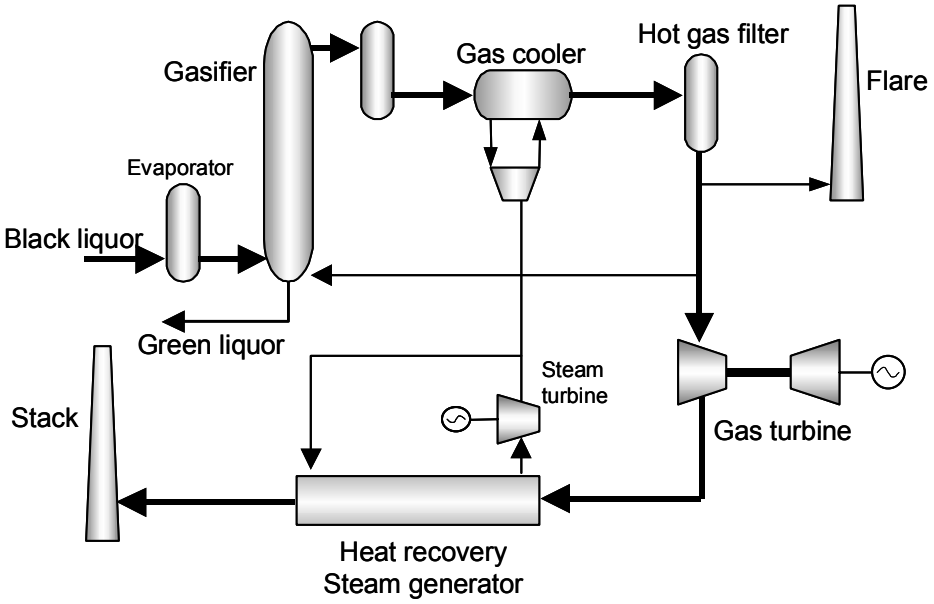

Figure 1.7: Integrated gasification and combined cycle (IGCC) [62]

In the gasifier, the organic matter in black liquor is partially oxidized with an oxidizing agent (O_2, CO_2, or H_2O) to form syngas, while leaving behind a condensed

phase. The syngas is cleaned to remove particulates and tars and to absorb inorganic species (i.e., alkali vapor species, SO_2, and H_2S), and this is done to prevent damage to the gas turbine and to reduce pollutant emissions. The clean syngas is burned in gas turbines coupled with generators to produce electricity, and gas turbines are inherently more efficient than the steam turbines of recovery boilers due to their high overall air-fuel ratios [50]. The hot exhaust gas is then passed through a heat exchanger (typically a waste-heat boiler) to produce high-pressure steam for a steam turbine and/or process steam. The condensed phase (smelt) continuously leaves the bottom of the gasifier and must be processed further in the lime cycle to recover pulping chemicals.

In recovery boilers, essentially all of the alkali species and sulfur species leave in the smelt (mostly as Na_2S and Na_2CO_3), but in gasifiers, there is a natural partitioning of sulfur to the gas phase (primarily H_2S) and alkali species to the condensed phase after the black liquor is gasified. Because of this inherent separation, it is possible to implement alternative pulping chemistries that would yield higher amounts of pulp per unit of wood consumed [37, 40]. Gasification at low temperatures thermodynamically favors a higher sodium/sulfur split than gasification at high temperatures, which results in higher amounts of sulfur gases at low temperatures. Because a large amount of the black liquor sulfur species leaves the low-temperature process as H_2S, H_2S may be recovered via absorption to facilitate alternative pulping chemistries. Industry has numerous patented processes for accomplishing the absorption, including using green or white liquor as an absorbing solvent [37, 40, 47].

The partitioning of sodium and sulfur in black liquor gasification requires a higher capacity for the lime cycle compared to the current technology. The sodium/sulfur split results in a higher amount of Na_2CO_3 in the green liquor because less sulfur is available in the smelt to form Na_2S. For each mole of sulfur that goes into the gas phase, one more mole of Na_2CO_3 is formed in the condensed phase [37]. The increase in Na_2CO_3 results in higher causticization loads, increases in lime kiln capacity, and increases in fossil fuel consumption to run the lime kiln. This leads to higher raw material and operating costs, which must be reduced in order to make the gasification process economically favorable. Non-conventional cost-reducing processes for causticization, particularly those motivating the work in this thesis, will be discussed in Chapter 2.

Black liquor gasification may be performed either at low temperatures or at high temperatures, based on whether the process is conducted above or below the melting temperature range (650-800°C) of the spent pulping chemicals [62]. In low-temperature gasification, the alkali salts in the condensed phase remain as solid products while molten salts are produced in high-temperature gasification. Low-temperature gasification is advantageous over high-temperature gasification because gasification at low temperatures yields improved sodium and sulfur separation. Additionally, low-temperature gasification requires fewer constraints for materials of construction because of the solid product. However, the syngas of low-temperature gasification may contain larger amounts of tars, which can contaminate gas clean-up operations in addition to contaminating gas turbines upstream of the gasifier. These contamination problems can result in a loss of fuel product from the gasifier. [62].

1.6. Environmental and Societal Impact of Black Liquor Gasification

Whether it is conducted at high or low temperatures, black liquor gasification is still superior to the current recovery boiler combustion technology. The thermal efficiency of gasifiers is estimated to be 74% compared to 64% in modern recovery boilers, and the IGCC power plant could potentially generate twice the electricity output of recovery boiler power plants given the same amount of fuel [21]. While the electrical production ratio of conventional recovery boiler power plants is 0.025-0.10 MW_e/MW_t, the IGCC power plant can produce an estimated 0.20-0.22 MW_e/MWt [21, 62]. This increase in electrical efficiency is significant enough to make pulp and paper mills potential exporters of renewable electric power. Alternatively, pulp mills could become manufacturers of biobased products by becoming biorefineries.

Additionally, the new technology could potentially save more than 100 trillion BTU's of energy consumption annually, and within 25 years of implementation, it could save up to 360 trillion BTU/year of fossil fuel energy [37]. The new technology also offers the benefits of improved pulp yields if alternative pulping chemistries are included, and reductions in solid waste (i.e., ash from consumed biomass) discharges. Also, the process is inherently safer because the gasifier does not contain a bed of char smelt unlike in recovery boilers, which reduces the risk of deadly smelt-water explosions [62].

IGCC power plants will reduce wastewater discharges at pulp and paper mills, even though they most likely will not significantly impact water quality [37]. Also, IGCC power plants will reduce cooling water and make-up water discharges locally at the mill, and because the efficient gasifiers will cause grid power reductions,

substantial reductions in cooling water requirements at central station power plants will also occur [37]. Central station power plants have large water requirements for cooling towers in order to provide grid power to customers. Overall, the implementation of IGCC power plants will cause net savings in cooling water requirements and net reductions in wastewater discharges.

The most significant environmental impact caused by black liquor gasification will occur in air emissions. Compared to the current recovery technology, the IGCC system could cause low emissions of many pollutants, such as SO_2, nitrogen oxides (NO_x), CO, VOC's, particulates, and TRS gases, and overall reductions in CO_2 emissions. Even with improved add-on pollution control features, the recovery boiler system still causes higher overall emissions than the IGCC system [37-40]. Table 1.1 shows a list of different emissions and their qualitative environmental impact, along with relative emissions rates for both recovery boilers and gasifiers:

Table 1.1: Relative emissions rates of different emissions [37]

Pollutant	Relative Environmental Impact	Relative Emissions Rates with Controls on Recovery Boilers	Relative Emissions Rates with Gasification Technology
SO_2	High	Low	Very Low
NO_X	High	Medium	Very Low
CO	Low	Medium	Very Low
VOC's	High	Low	Very Low
Particulates	High	Low-Medium	Very Low
CH_4	Low-Medium	Low	Very Low
HAP's	Medium-High	Low	Very Low
TRS	Low	Low	Very Low
Wastewater	Medium-High	Low	Very Low-Low
Solids	Very Low	Low	Low

Because the biomass sources at pulp and paper mills are sustainably grown, a black liquor gasification based IGCC plant or biorefinery would transfer smaller amounts of CO_2 to the atmosphere as compared to using fossil fuels. As seen in Figure 1.1, the vast majority of the CO_2 emitted would be captured from the atmosphere for photosynthesis and used for replacement biomass growth, producing O_2 [37]. According to Larsen, if the pulp and paper industry converts the 1.6 quads of total biomass energy to electricity, 130 billion kWh/year of electricity could be generated. This electricity generation in a black liquor gasification based IGCC plant could displace net CO_2 emissions by 35 million tons of carbon per year within 25 years of implementation [37]. Within 25 years of implementation, the IGCC could displace 160,000 net tons of SO_2, since most of the SO_2 produced in the process would be absorbed during H_2S recovery [37]. Moreover, the overall reduction of TRS gases (i.e., H_2S) using gasification technology will also reduce odor, which will improve public acceptance of pulp and paper mills, particularly in populated areas.

Clearly, black liquor gasification technology offers tremendous potential to make an impact on society. However, before it can totally replace the current recovery boiler technology, some work must be done to make it more economically attractive. One major area that requires attention is the causticization process. Gasification technology can cause significant increases in capacity for the lime cycle, requiring significant increases in fossil fuel consumption, and to improve economic viability, alternative causticization technologies must be considered. These causticization technologies will be explored in Chapter 2, leading to the experimental work conducted in this thesis.

1.7. Thesis Objectives

The primary objective of this thesis is to investigate the effects of high-temperature gasification process conditions (residence time, temperature, gas environment) on hydroxide formation in the condensed phase product, using a mixture of H_2O and CO_2 as gasifying agents. As seen in Chapter 2, many investigations have been undertaken on causticization processes that rely on additional chemicals, but few, if any, investigations have involved causticization processes that do not use additional chemicals. With the results in this work, it is possible to determine the feasibility of a causticization process that does not require additional chemicals. If proven feasible, this process could provide another energy-efficient alternative to the traditional lime cycle and could contribute to the economic attractiveness of black liquor gasification technology.

In addition to investigating hydroxide formation, this thesis project will also further the understanding of carbon species transformations that occur during kraft

black liquor gasification. In doing so, this thesis will investigate the effects of H_2O and CO_2 on the carbon gasification rate and the split of sulfur between the condensed-phase and gas-phase products. The results will provide new fundamental information, as data illustrating the effects of two different, competing oxidizing agents on gasification processes do not exist in the research literature.

Finally, this project will use recently developed analysis techniques to obtain data for char yields and hydroxide formation. These new techniques are relatively simple and are proven to be advantageous over traditional analysis methods. These techniques, in addition to other techniques used in this thesis, will be discussed in Chapter 3.

CHAPTER 2

RELEVANT THEORY AND LITERATURE REVIEW

2.1. Background

Black liquor gasification in pulp and paper mills offers potential to make a significant economic and environmental impact on society. Before black liquor gasifiers can totally replace the current recovery boiler technology, additional process modifications must be done to make the overall concept more economically attractive. One major area of concern is the conventional causticization process, which requires increased capacity and increased fossil fuel consumption upon implementation of gasifiers.

Non-conventional causticization processes motivating the work in this thesis have been considered, and they will be explored in this chapter. Before these alternative processes are explored, this chapter will provide the theoretical underpinnings of the black liquor pyrolysis and gasification processes, and the processes by which certain chemical species, such as carbonate and alkali metal vapors, are formed. Additionally, this chapter will briefly discuss sulfur species transformations that occur in black liquor gasification, and it will provide terminology that will be used in future chapters of this thesis.

2.2. Black Liquor Thermal Conversion

In general, the basic thermochemical conversion of black liquor solid droplets can be separated into four, often overlapping, stages similar to those for the

combustion of other solid and liquid fuels. These four stages - drying, devolatilization, char burning, and smelt reactions - are illustrated in Figure 2.1:

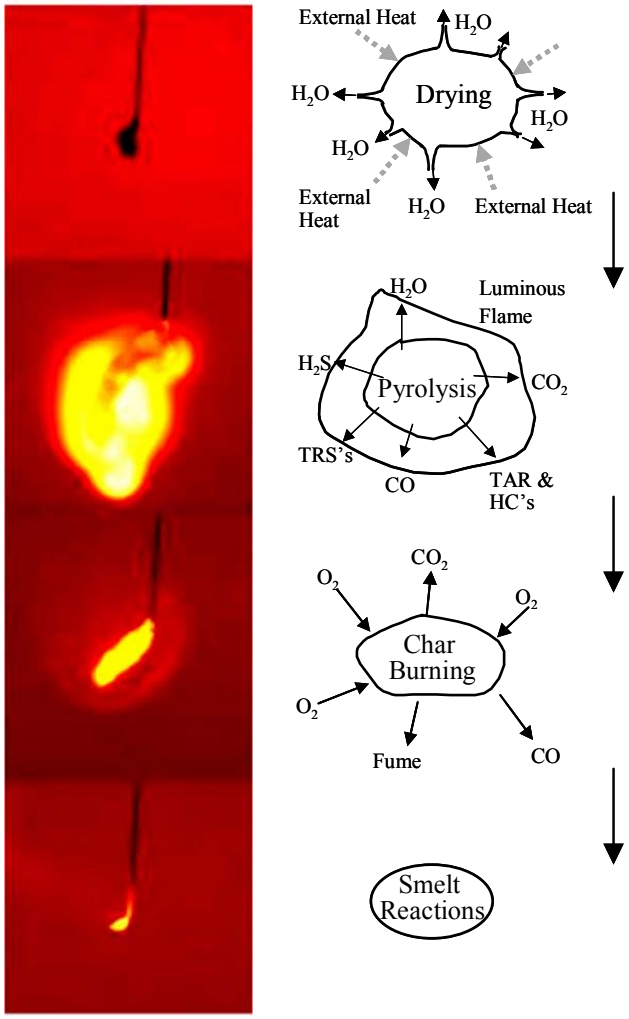

Figure 2.1: Black liquor droplet thermal conversion [62]

During the drying process, external heat vaporizes liquid water contained in the droplet. The droplet swells, and the porous surface ruptures as a result of the vaporization. Most of the water escapes the droplet before the other stages of thermal conversion begin [62].

In the devolatilization process, the organic matter in black liquor solids begins to decompose thermally above 200°C, producing water vapor, CO_2, CO, H_2, condensable organic compounds (tars), light hydrocarbons (i.e., CH_4 and C_2H_2), and light sulfur gases such as H_2S and SO_2 [29-30, 62, 64-65, 67]. The devolatilization process is essentially complete starting at temperatures of 650-750^oC, with most mass loss occurring very early in the process [27, 32, 58, 62, 67]. During the thermal breakdown of the organic matter, the black liquor droplet swells even more in order to allow for releasing the gases. The volume of the droplet typically increases by a factor of 3-4, sometimes higher, during devolatilization [32, 46, 71].

The remaining black liquor solids after devolatilization are known as *char residue*, which consists of ash and residual organic carbon or fixed carbon, some hydrogen, and most of the inorganic matter from the pulping chemicals. The ash-free char residue is referred to as *char*, and the carbon remaining as carbonate in the char residue is referred to as *carbonate carbon*. Moreover, the sum of fixed and carbonate carbon is referred to as *total carbon*. If devolatilization occurs in an inert (i.e., N_2) atmosphere, it is referred to as *pyrolysis*. This term often incorporates solids heating and organic matter breakdown after devolatilization as well [62].

During char burning, or char gasification, the size of the swollen char residue decreases considerably, and fixed carbon in the char is further oxidized by oxygen donor gases, such as CO_2 and H_2O, to form CO and CO_2. In a recovery boiler, black liquor char collects at the bottom of the boiler to form the char bed, where most of the oxidation occurs. The inorganic matter in the char bed is melted to form a smelt, and as the oxidation proceeds, the smelt reactions occur. Residual sulfur species are

reduced mainly to sulfide species, while residual alkali species are converted primarily to carbonate species. Similar inorganic reactions occur in black liquor gasifiers, but with a natural split occurring between the sulfur species in the product gas and the alkali species in the char.

In the work of Hupa et al., a typical time-series droplet diameter profile for a large black liquor droplet (initial diameter = 1.7 mm) burning in air at 700°C was shown:

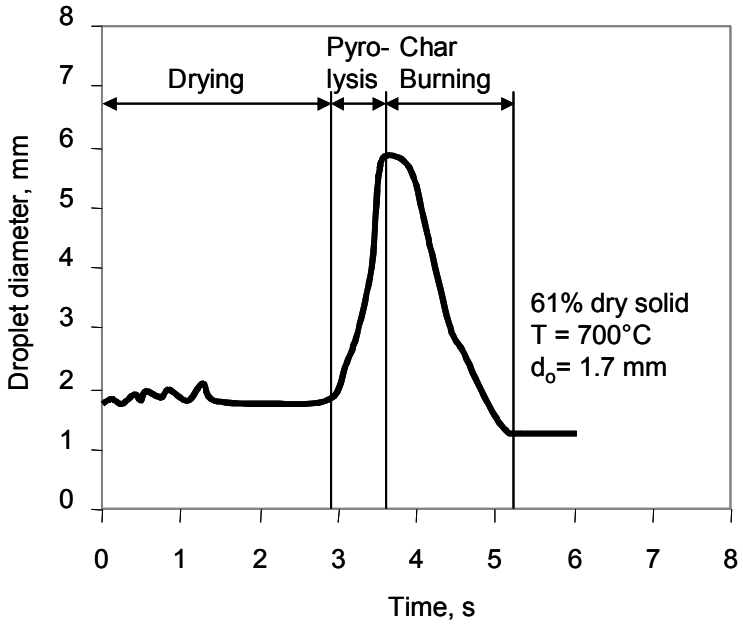

Figure 2.2: Average droplet diameter during black liquor combustion [32]

Verrill and Wessel developed a model in 1995 that accounts for swelling behavior in black liquor solid droplets. Figure 2.3 shows a profile of predicted particle diameter for small-diameter droplets (diameter = 100 μm) with respect to exposure time in an entrained-flow furnace during combustion in a pure N_2 environment:

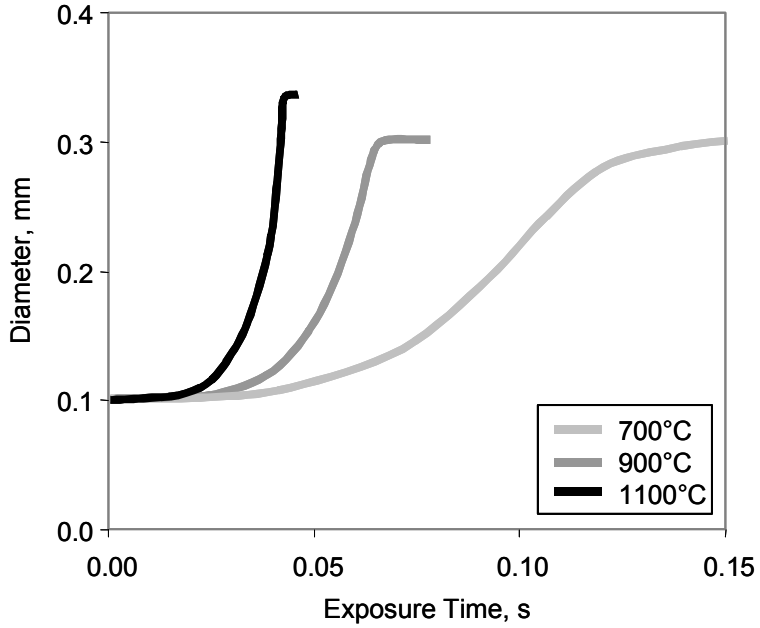

Figure 2.3: Predicted swelling behavior for black liquor solids of 100 μm initial diameter, in pure N_2 [71]

Particle swelling is a complicated process, involving complex simultaneous heat and mass transfer processes, but it is an important consideration in modeling the behavior of black liquor solids in a gasifier or recovery boiler. In addition to the work of Verrill and Wessel, several efforts have been undertaken to simulate the behavior of the particles while accounting for swelling [46, 61]. For example, Jarvinen has recently developed a detailed swelling droplet model for devolatilization, with experimental validation [35]. Also, a computational fluid dynamics program that models black liquor combustion has been developed for the entrained-flow gasifier used in this thesis. More details on this program will be given in Chapter 3.

2.3. Fundamentals of Black Liquor Gasification

Technically, the term *gasification* refers to the overall thermochemical

conversion of organic material (primarily elemental carbon) to CO or CO_2 in the presence of an oxygen donor gas, such as H_2O, CO_2, or O_2. During the thermochemical conversion, devolatilization occurs, producing a product gas, while leaving behind char residue. The purpose of gasification is to produce product gases via partial oxidation of the combustible material. In combustion, on the other hand, the purpose is to obtain the maximum amount of heat in the product gases by completely oxidizing the combustible material [21, 62]. The key reactions taking place during gasification and their kinetic and thermodynamic behavior are shown in Table 2.1:

Table 2.1: Reactions that occur during gasification [2-3, 24, 62]

Reaction	**Equilibrium conditions**		**Kinetics (rate of reaction)**	**Heat of reaction**
	Effect of increase in temperature	**Effect of increase in pressure**		
Solid-gas				
$C+½O_2 \leftrightarrow CO$ (partial combustion)	to left	to left	fast	exothermic
$C+O_2 \rightarrow CO_2$ (combustion)	-	-	very fast	exothermic
$C+CO_2 \leftrightarrow 2CO$	to right	to left	slow	endothermic
$C+H_2O \leftrightarrow CO+H_2$ (water-gas)	to right	to left	moderate	endothermic
$C+2H_2 \leftrightarrow CH_4$ (hydrogasification)	to left	to right	slow	exothermic
Gas-gas				
$CO+H_2O \leftrightarrow CO_2+H_2$ (water-gas shift reaction)	to left	-	moderate	exothermic
$CO+3H_2 \leftrightarrow CH_4+H_2O$	to left	to right	slow	exothermic

The rapid heating and devolatilization at the onset of the gasification process provide the heat required to induce the endothermic reactions in Table 2.1. The reactions taking place during gasification are quite sensitive to changes in temperature and pressure, and for the most part, they are exothermic. High temperatures and low

pressures (i.e., atmospheric pressure), such as those used in this thesis, favor gasification reactions.

The basic overall reactions for gasification in the presence of CO_2 and H_2O are as follows:

$$C + CO_2 \rightarrow 2CO \quad (2.1)$$

$$C + H_2O \rightarrow CO + H_2 \quad (2.2)$$

Previous studies have shown that these reactions are catalyzed by the alkali metals present in black liquor [48-49]. These alkali metals are part of the inorganic salts from pulping and also serve as counter ions to dissolved organic anions resulting from the degradation of cellulose, lignin, and hemicellulose. During gasification, some of the alkali metals go into the product gas, but most of the alkali metals become associated with organic functional groups on the char carbon. Previous work has shown that the functional groups produced during alkali-catalyzed gasification are mainly in the form of carboxylate and phenolate moieties [10, 48-49]. The alkali carboxylates, such as formic acid and acetic acid, originate from hemicellulose and cellulose (polysaccharides), and alkali phenolates originate from lignin [72]. Figure 2.4 shows the basic interaction of alkali metals with the functional groups on char surfaces:

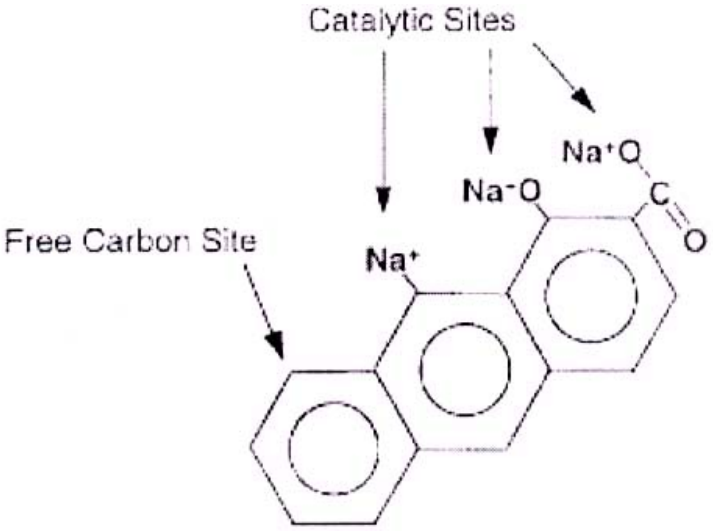

Figure 2.4: Association of alkali metals with functional groups on char surfaces [72]

Basically, the carboxylate and phenolate moieties are sites for exchange of oxygen atoms with H_2O and CO_2, and they serve as intermediates in the alkali-catalyzed gasification of carbon [10]. They are stable in the presence of oxidizing gases.

The mechanism for alkali-catalyzed carbon gasification is driven by an oxidation-reduction cycle in which the oxygen donor gas is transferred to carbon active sites through the catalytically active alkali species [13-14]. The mechanism is currently known to occur in a 4-step reaction sequence in which the oxidizing agent (CO_2, for example) is first adsorbed onto an unoxidized active site:

$$CO_2 + * \leftrightarrow *CO_2 \qquad (2.3)$$

The adsorbed CO_2 decomposes, resulting in gaseous CO and an oxidized catalyst site, *O:

$$*CO_2 \leftrightarrow *O + CO \tag{2.4}$$

Oxygen is then transferred from the oxidized catalyst site to a neighboring free carbon site (C_f) to form a carbon-oxygen complex (C(O)). Finally, this complex decomposes to form CO and re-generates a free carbon site for further gasification:

$$*O + C_f \rightarrow * + C(O) \tag{2.5}$$

$$C(O) \rightarrow CO + C_f \tag{2.6}$$

The mechanism for H_2O gasification occurs in the same manner as CO_2 gasification in Equations 2.3-2.6 [42].

The activation energy for the rate of CO_2 gasification for black liquor char is 205 kJ/mol [26]. Similarly, the activation energy for the rate of H_2O gasification is 210 kJ/mol [42]. Previous work has demonstrated that the rates of reaction for steam and CO_2 gasification take the following form, known as Langmuir-Hinshelwood kinetics [41-42]:

$$r = \frac{-K[H_2O]}{1 + K_{H_2O}[H_2O] + K_{H_2}[H_2]} \tag{2.7}$$

$$r = \frac{-K[CO_2]}{1 + K_{CO_2}[CO_2] + K_{CO}[CO]} \tag{2.8}$$

Previous work has shown that CO suppresses the rate of CO_2 gasification, while the addition of H_2 suppresses the rate of H_2O gasification [2-3, 26, 28]. Moreover, in the case of CO_2 gasification, previous work has shown that the rate of gasification increases as CO_2, increases, but at high levels of CO_2, the rate plateaus

and does not increase further. This is the result of saturated active sites limiting catalytic activity and preventing higher gasification rates [26, 28].

2.4. Formation and Destruction of Carbonate During Black Liquor Gasification

During gasification, most of the alkali species in the char residue are ultimately converted to carbonate species via organic and inorganic processes. The alkali carboxylate and phenolate moieties are stable in the presence of oxidizing gases, as these gases replace the oxygen consumed by gasification. As gasification continues and char carbon becomes depleted, the moieties are converted to carbonate species. However, in the absence of oxidizing gases, the moieties are converted to unstable alkali carbide species, which causes volatilization of the alkali metals and a loss of catalytic activity. Wåg has proposed a framework for the formation of carbonate and alkali metal vapors in gasification while considering char residue reactions and the interaction of alkali metal salts in the organic matter:

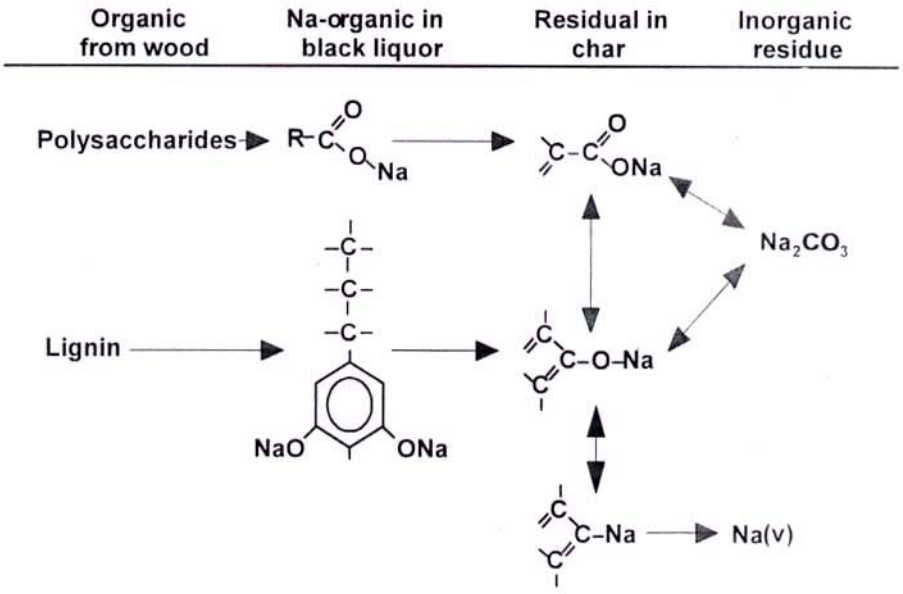

Figure: 2.5: Proposed mechanism for formation and interaction of carboxylate and phenolate sites during combustion of black liquor, and their oxidation-reduction pathways [72]

In addition to organic pathways, alkali carbonate is also produced from inorganic reactions, particularly inorganic sulfur reactions, in black liquor char. Because of the inherent separation of sulfur and alkali species during gasification, only a small amount of sulfur species remain in the char residue, but they do affect carbonate formation. Sulfur species transformations occur during devolatilization and gasification, with the most notable transformation involving sulfate reduction to sulfide in the char [9, 56, 68-69]. The sulfate reduction reactions cause further reductions of char residue mass as they convert fixed carbon to CO and CO_2:

$$2C + Na_2SO_4 \rightarrow Na_2S + 2CO_2 \qquad (2.9)$$

$$4C + Na_2SO_4 \rightarrow Na_2S + 4CO \qquad (2.10)$$

Reactions of alkali sulfur species with CO_2 and H_2O also cause carbonate formation. The char sulfide species from sulfate reduction react with the oxidizing agents to form carbonate, while some residual sulfate, thiosulfate, and sulfite species, which have not been reduced to sulfide, also form carbonate [29, 62, 67, 69]:

$$Na_2S + 2HCO_2H \rightarrow Na_2CO_3 + H_2S + CH_2O \quad (2.11)$$

$$Na_2S + 2CO_2 \rightarrow Na_2CO_3 + COS \quad (2.12)$$

$$Na_2S + H_2O + CO_2 \rightarrow Na_2CO_3 + H_2S \quad (2.13)$$

$$Na_2S_2O_3 + CO_2 \rightarrow Na_2CO_3 + SO_2 + S \quad (2.14)$$

$$Na_2SO_4 + CO \rightarrow Na_2CO_3 + SO_2 \quad (2.15)$$

$$3Na_2SO_4 + CO_2 \rightarrow 4Na_2CO_3 + 4SO_2 \quad (2.16)$$

$$Na_2SO_3 + CO_2 \rightarrow Na_2CO_3 + SO_2 \quad (2.17)$$

Previous work has shown that Equation 2.13 is the most important carbonate formation reaction [66]. The thiosulfate reaction in Equation 2.14 is not very important during the high-temperature conditions considered in this thesis, as thiosulfate decomposes rapidly starting at 700°C. Also, the sulfate and sulfite reactions in Equations 2.15-2.17 are plausible, but with their rates being slower than the sulfide reaction rates of Equations 2.11-2.13, they too are not very important [62, 66].

The presence of CO_2 and H_2O causes an increase in carbonate formation (i.e., Equation 2.13) in the char at intermediate gasification residence times and high temperatures compared to pyrolysis conditions. However, at temperatures above

1000°C and at high gasification residence times, the amount of carbonate in the char decreases considerably. This is due to carbonate destruction reactions that occur as the catalytic active sites become depleted during gasification [63]:

$$C + Na_2CO_3 \rightarrow 2Na(v) + CO_2 \qquad (2.18)$$

Previous work has shown that carbonate formation reaches a maximum level at intermediate residence times and at 700-900°C, because the conditions are favorable for oxidation of char carbon. The oxidizing gases adsorb onto the active sites to cause char oxidation, and then they readsorb onto other activated sites for further oxidation of char carbon. The rates of char oxidation and readsorption are similar to each other during these gasification conditions. However, at long residence times and at temperatures above 1000°C, it is apparent that the rate of char carbon oxidation exceeds the rate of readsorption of the oxidizing gases, and this leads to carbonate destruction and alkali metal vapor formation [63].

The presence of CO_2 or H_2O not only causes higher levels of carbonate in the char at high temperatures and intermediate residence times, but it also reduces the carbonate destruction that occurs at high temperatures and high residence times. After measuring alkali species (sodium and potassium) in the char, it was determined that the presence of CO_2 and H_2O reduces alkali metal volatilization [58, 63, 66, 71]. The oxidizing gases maintain stable active sites for carbon gasification, and the absence of oxidizing gases leads to unstable alkali carbide active sites and alkali metal vapor formation, as seen in Figure 2.5. Previous work has shown that the sodium and potassium remaining in char at long residence times and high temperatures are the

highest in the presence of H_2O/N_2 mixtures, but very high levels also remain in mixtures of CO_2 and N_2 [33, 66].

2.5. Conventional and Non-Conventional Causticization

Figure 1.6 shows the traditional causticization process for producing white liquor in pulp and paper mills. The overall purpose of conventional causticization is to convert the alkali carbonate species in green liquor (black liquor smelt dissolved in water) to hydroxide, which can then be re-used in pulping. A summary of the key reactions in conventional causticization is as follows:

$$CaCO_3(s) \leftrightarrow CaO(s) + CO_2(g) \qquad (2.19)$$

$$CaO(s) + H_2O \leftrightarrow Ca(OH)_2(s) \qquad (2.20)$$

$$Ca(OH)_2(s) + Na_2CO_3(aq) \leftrightarrow 2NaOH(aq) + CaCO_3(s) \qquad (2.21)$$

Equation 2.20 is referred to as the *slaking reaction*, which uses CaO produced from a lime kiln. Equation 2.21 is often referred to as the *causticizing reaction*, and Equation 2.19 is often referred to as the *calcination reaction*. The lime product of the slaking reaction reacts with aqueous carbonate in green liquor to form the hydroxide of white liquor and $CaCO_3$, which is referred to as *lime mud*. The lime mud is separated from the white liquor by sedimentation and filtration, and it is washed and sent back to the lime kiln to produce more CaO. The completeness of the reversible causticizing reaction in Equation 2.21 is known as *causticizing efficiency*, and the causticizing efficiency varies from 80-90% depending on sulfur and alkali species concentrations, and excess lime [51-52]. The unconverted alkali carbonate is

known as *dead load*, and it is desirable to minimize dead load formation for efficient operation of the lime cycle.

As mentioned previously, the lime cycle is an energy-intensive process, requiring high capital costs. The calcination reaction occurring in the lime kiln is endothermic and occurs at 850-900^{o}C, requiring external heat from non-renewable fuels. However, the causticization and slaking reactions are exothermic and occur at around 100^{o}C. With energy being delivered at high temperatures and then released at low temperatures, the energy economy of the lime cycle is inherently low [51]. Moreover, because the causticizing efficiency is 80-90%, significant dead load is produced in the lime cycle, requiring increased energy consumption in the other parts of the kraft process. Furthermore, as mentioned in Chapter 1, the implementation of black liquor gasifiers will increase the capacity of the lime cycle because the natural sodium/sulfur split that occurs in gasification produces a higher amount of carbonate in the char than in combustion.

The drawbacks mentioned above are major driving forces for developing non-conventional causticization technologies. Research and development of alternative causticization technologies began in Finland in the 1970's, and interest in these technologies continues today, especially in conjunction with black liquor gasification research [51]. The key concept behind these technologies is to add an amphoteric metal oxide or salt to the combustion process, which will convert molten alkali carbonate to alkali oxide and CO_2 under combustion conditions. This conversion process is known as *decarbonization*, and the amphoteric metal oxide is

referred to as the *decarbonizing agent*. Upon dissolution in water, the resultant smelt produces white liquor directly, without the use of the lime cycle.

Non-conventional causticization technologies are separated into two categories based on the water solubility of the decarbonizing agent: *autocausticization* and *direct causticization*. Autocausticization occurs when the reaction product is soluble in water, and the decarbonizing agent goes through the pulping and chemical recovery processes as a caustic solution [54-55]. Direct causticization occurs when the reaction product is insoluble in the caustic solution, and the decarbonizing agent must be separated from the solution and not carried through the kraft process [51]. The term *in-situ causticization* refers to both autocausticization and direct causticization processes, and this term is used extensively throughout the research literature.

Because the decarbonizing agents travel through both the pulping and chemical recovery processes during autocausticization, they are regarded as part of the pulping chemistry. To be effective in pulping, the decarbonizing agents must be very alkaline, in addition to being effective in decarbonization [51]. Total autocausticization is attractive, but it requires large amounts of chemicals (i.e., decarbonizing agents) to venture through the process, and it produces large amounts of inactive pulping chemicals and dead load. Partial causticization, which involves an optimal mixture of smaller-scale autocausticization and conventional lime burning processes, is more attractive in that it reduces the dead load, even though it still requires external heat sources to run the lime cycle. Several decarbonizing agents (i.e., B_2O_3, P_2O_5, SiO_2, and Al_2O_3) have been investigated for all types of black liquor

combustion systems, and Nohlgren expounds on them [51]. The most attractive autocausticizing agent involves alkali borates, such as $NaBO_2$, and the overall borate autocausticization reactions are summarized as follows:

$$NaBO_2 + Na_2CO_3 \leftrightarrow Na_3BO_3 + CO_2 \quad (2.22)$$

$$Na_3BO_3 + H_2O \rightarrow 2NaOH + 2NaBO_2 \quad (2.23)$$

Previous work shows that the use of borates is favorable for partial autocausticization on a large scale, using recovery boilers. Borate autocausticization during black liquor gasification has been investigated as well, but further research must be done to prove its feasibility [51, 53, 54-55].

Direct causticization systems use insoluble metal oxides for decarbonizing agents, such as TiO_2, Fe_2O_3, and Mn_2O_3. These metal oxides form insoluble products, which must be removed from the caustic solution in a solid separation system before being recycled back to the black liquor combustion process. Unlike autocausticizing agents, direct causticizing agents do not participate in pulping, and the direct causticizing agents remain in the solid phase during black liquor combustion temperatures [52]. While requiring solids separation and a high circulation of solids, direct causticization systems eliminate the lime cycle unlike in partial autocausticization systems. Additionally, they yield improved causticizing efficiency and energy economy, and lower amounts of dead load compared to autocausticization systems.

Numerous studies have been carried out on direct causticization reactions with titanates (TiO_2) [51-52, 60]. The reaction between alkali carbonate and TiO_2

yields various alkali titanates during the causticization reactions. Previous work has shown that the most prominent decarbonizing reactions involve trititanate and pentatitanate compounds:

$$3TiO_2 + Na_2CO_3 \leftrightarrow Na_2O \cdot 3TiO_2(s) + CO_2 \quad (2.24)$$

$$5(Na_2O \cdot 3TiO_2) + 7Na_2CO_3 \leftrightarrow 3(4Na_2O \cdot 5TiO_2)(s) + 7CO_2 \quad (2.25)$$

Other decarbonizing reactions are theoretically possible and have been explored in earlier studies [18, 52, 54-55]. The hydrolysis reactions for the trititanate and pentatitanate compounds are as follows:

$$3(4Na_2O \cdot 5TiO_2) + 7H_2O \rightarrow 14NaOH(aq) + 5(Na_2O \cdot 3TiO_2)(s) \quad (2.26)$$

$$2(Na_2O \cdot 3TiO_2) + H_2O \rightarrow 2NaOH(aq) + Na_2O \cdot 6TiO_2(s) \quad (2.27)$$

The hexatitanate product compound in Equation 2.27 can be converted to trititanate in decarbonizing reactions along with the decarbonizing reactions in Equations 2.24-2.25 [52]. These polytitantate compounds are recycled back to the combustion process for further hydroxide formation. While these compounds are suitable for kraft pulping systems, they are problematic in recovery boilers because they cause high char melting points, which prevents smelt formation [51]. However, they appear to be suitable for black liquor gasification, particularly in entrained-flow reactors, but more research must be done to prove feasibility [51-52, 73].

Ferric oxide (Fe_2O_3) has also been considered as a possible direct decarbonizing agent. The decarbonizing and hydrolysis reactions are as follows:

$$Fe_2O_3 + Na_2CO_3 \rightarrow 2NaFeO_2 + CO_2 \quad (2.28)$$

$$2NaFeO_2 + H_2O \rightarrow 2NaOH + Fe_2O_3 \quad (2.29)$$

Ferric oxide is an effective decarbonizing agent, but it is not suitable for the kraft process [51]. However, it is still suitable for pulp and paper mills that use non-conventional pulping chemistries. For example, the first commercial direct causticization process, known as the Direct Alkali Recovery System (DARS), successfully uses ferric oxide [15-16, 51]. The pulping process for the DARS uses soda-anthraquinone chemistry, which differs from the chemistry of the kraft process, and the decarbonizing reaction occurs in a fluidized bed. After decarbonization, the white liquor is leached from the solid product downstream [15-16, 17]. The process offers high causticizing efficiencies (92-94%), eliminates the lime cycle, and offers similar advantages offered by black liquor gasification (i.e., low smelt-water explosion risk) [51].

Unlike ferric oxides, manganese oxides (Mn_2O_3) can potentially be used in the kraft process and in black liquor gasifiers. Previous work has shown that by using MnO_2, Mn_3O_4 is formed after heating to black liquor combustion temperatures. The reactions for decarbonization and hydrolysis involving Mn_3O_4 are as follows [51]:

$$Mn_3O_4 + Na_2CO_3 \rightarrow 2NaMnO_2 + MnO + CO_2 \quad (2.30)$$

$$2NaMnO_2 + MnO + H_2O \rightarrow 2NaOH + Mn_3O_4 \quad (2.31)$$

Like the titanate direct causticizing agents, more research must be done with manganese oxide direct causticizing agents to confirm their feasibility in black liquor gasification systems.

One major objective of this thesis is to investigate the possibility of a non-conventional causticization process that uses neither a causticizing agent nor the lime cycle. While several feasibility studies of alternative causticization processes with chemical agents have been undertaken, few efforts, if any, have been made thus far to determine the feasibility of a causticization process that does not require additional chemicals.

It is theoretically possible to develop a gasification unit, coupled with a causticization unit that does not require lime burning or external chemicals. A conceptual schematic of such a process, utilizing two gasification stages, is as follows:

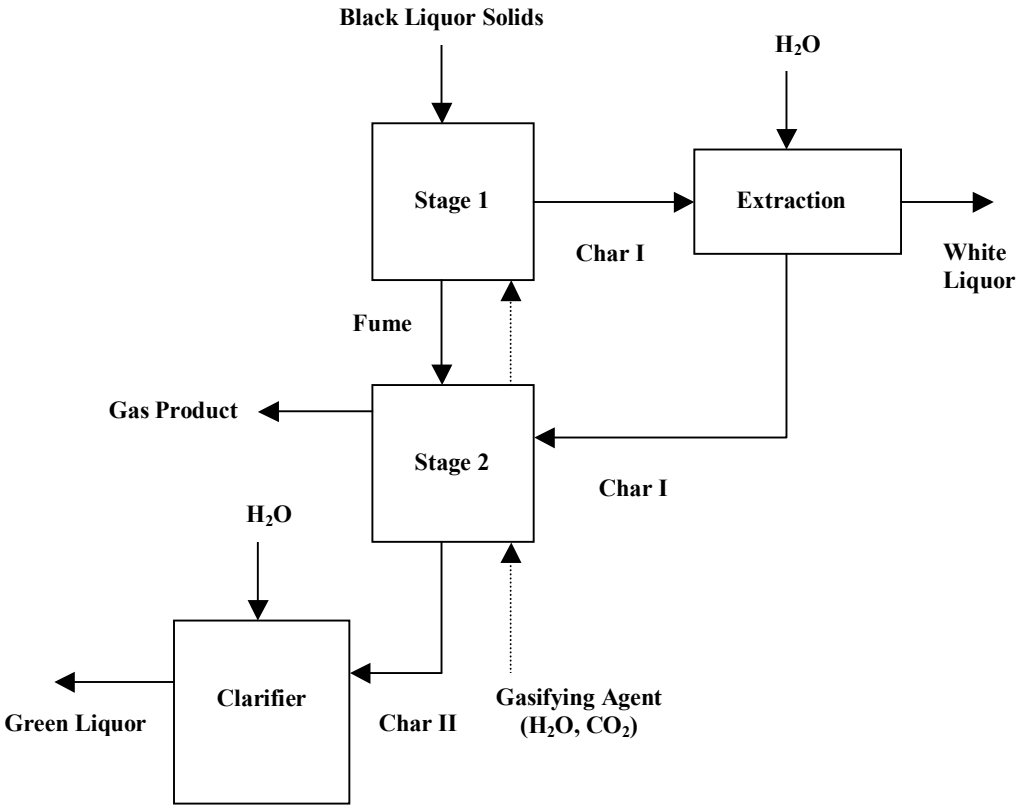

Figure 2.6: Schematic diagram of a potential 2-stage gasification and causticization system

In a 2-stage process, the black liquor solids enter the first gasifier stage and undergo devolatilization, and after this stage, a large amount of the char may not have been completely converted to carbonate. Through the interactions of the catalytic moieties during gasification in Figure 2.5, it is possible to produce significant amounts of hydroxide directly with water after the first stage. Thus, a large amount of char is sent from the first stage to an extraction system, where water converts unconverted phenolate moieties to hydroxide. The remainder of the solid char, along with fume and product gases from the first stage, enters the second stage for further gasification and inorganic smelt reactions, and the char residue from this stage is dissolved in a

clarifier to form green liquor. The green liquor can most likely be used in H_2S absorption, while the solid waste from the clarifier can be processed further downstream for other applications.

This process, if proven feasible in this work, offers the potential to maximize white liquor production without using causticizing agents or the lime cycle. At the very least, partial causticization could be accomplished without the aid of causticizing agents. Additionally, it may be possible to conduct the gasification-causticization process with one stage instead of two stages. Nevertheless, whether it consists of one stage or two stages, the gasification unit will produce large amounts of clean syngas for the IGCC power plant or biorefinery applications. Additionally, H_2S absorption for use in creating alternative pulping chemistries (i.e., polysulfide white liquor) and syngas cleaning systems should be compatible with this process [37, 39].

CHAPTER 3

EXPERIMENTAL PLAN AND PROCEDURES

3.1. Experimental Plan and Residence Time Determination

This work focuses on high-temperature gasification in the presence of H_2O and CO_2 at a wide range of particle residence times in a laboratory-scale Laminar Entrained-Flow Reactor (LEFR). High-temperature gasification was considered due its practical importance. Moreover, while several studies have been conducted with pyrolysis, H_2O gasification, and CO_2 gasification conditions, few studies have been conducted with gasification in the presence of both CO_2 and H_2O. It was also hypothesized that a mixture of both components would be needed to obtain representative hydroxide production in a causticization process without the aid of causticizing agents.

Because of difficulties associated with the experimental and analytical techniques, the experimental conditions were chosen so that the impact of each independent variable (temperature, residence time, and gas environment) could be examined with a limited number of experiments. Also, to achieve statistical confidence, each run was conducted in duplicate, and some randomization was introduced in the order of residence times examined. The experimental runs were conducted at 900^{o}C and 1000^{o}C and with a gas composition of 80% N_2, 10% CO_2, and 10% H_2O, and the residence times ranged from 0.46 to 1.52 s. Table 3.1 shows the experimental matrix, and Table 3.2 shows the order of runs for this work:

Table 3.1: Matrix of experimental conditions, with $N_2/CO_2/H_2O$ gasification at each condition

	Temperature (^oC)	
Residence Time (s)	900	1000
0.457		*
0.467	*	
0.876		*
0.906	*	
1.36		*
1.42	*	
1.52	*	

Table 3.2: Order of experimental runs

Run #	**Residence Time (s)**	**Temperature (^oC)**
1	1.52	900
2	1.52	900
3	0.467	900
4	0.467	900
5	0.906	900
6	0.906	900
7	1.42	900
8	1.42	900
9	1.36	1000
10	1.36	1000
11	0.876	1000
12	0.876	1000
13	0.457	1000
14	0.457	1000

As mentioned in Chapter 2, black liquor thermochemical conversion is a fairly complex process, but attempts have been made to simulate it. For the LEFR used in this work, a computational fluid dynamics and heat transfer program has been developed to determine the residence time of black liquor droplets in the reactor. The program is based on a three-dimensional mathematical model developed by Flaxman

that accounts for momentum transport in the gas phase; the relative velocity of the particles and gas; and transport of energy by radiation and convection between the particles, the surrounding gases, and the reactor walls [22]. It was later modified to account for devolatilization and swelling of the dry black liquor solids during pyrolysis and gasification, and also to account for sulfur species transformations [36, 45]. Only the swelling was taken into account in the residence time calculations in this work.

The program calculates the residence time of the particles during their path in the heating zone, and the Appendix shows these calculations with input parameters relevant to this work. More details regarding this program and its comparison to the Verrill and Wessel program mentioned in Chapter 2 can be found in the works of Sricharoenchaikul [62, 67]. The variation in residence times between 900^{o}C and 1000^{o}C results from variations in the actual heating zone length, as predicted by the program.

3.2. Black Liquor Solids (BLS)

The black liquor used in this project was produced from a typical kraft pulping process and forwarded by the group of Larry Baxter at Brigham Young University. The liquor is derived from pine softwood, and an elemental analysis indicates that its composition is comparable to black liquor used in previous work:

Table 3.3: Black liquor elemental composition in various studies

Element	Elemental Composition (wt. %)			
Study	**This Work**	**Sricharoenchaikul [62]**	**Gairns, et al. [29]**	**Frederick et al. [27]**
Liquor Type	**Softwood Pine Kraft**	**Softwood Pine Kraft**	**Mixed Hardwood Kraft**	**Softwood Pine Kraft**
C	35.6	34.9	34.1	39.8
H	3.34	3.05	3.2	4.2
S	4.06	2.9	4.0	4.0
Na	18.8	22.65	19.7	15.5
K	1.5	0.62	3.0	0.07
Cl	0.1	0.67	0.53	0.33
O*	36.6	35.1	35.3	36

* by difference

Initially in the liquid phase, the black liquor was dried to produce the BLS for the experiments. The liquid substance, with an estimated solids content of 45%, was dried in a pilot-scale spray dryer used at the Institute of Paper Science and Technology. This spray dryer, manufactured by Anhydro (Attleboro Falls, MA), transferred the black liquor from an agitated feed tank to a rotary atomizer, and the rotary atomizer sprayed the liquor evenly into a heating zone. The heating occurred at 125^{o}C within the zone and produced mostly spherical solid particles, which are advantageous in gasifier feeding over non-spherical particles produced in oven drying and grinding [64-65]. The resulting BLS were then sieved through a No. 120 mesh screen and retained on a No. 170 mesh screen, yielding solid particles in the size range of 90-125 μm. This particle size range is comparable to that of previous studies, and it is necessary for efficient feeding.

3.3. The Use of the LEFR in the Study of Black Liquor Gasification

The gasification experiments were conducted in a laboratory-scale Laminar Entrained-Flow Reactor (LEFR) operating at atmospheric pressure. This type of reactor has been used for a wide variety of coal and biomass research applications for over a quarter of a century, and it offers two features that are important when obtaining fundamental gasification data: 1) it uses particles that are small enough so that temperature gradients within the particles are negligible, and 2) it provides very rapid heating [62, 64-65]. This reactor is shown schematically in Figure 3.1, along with a listing of the char analysis techniques used in this project:

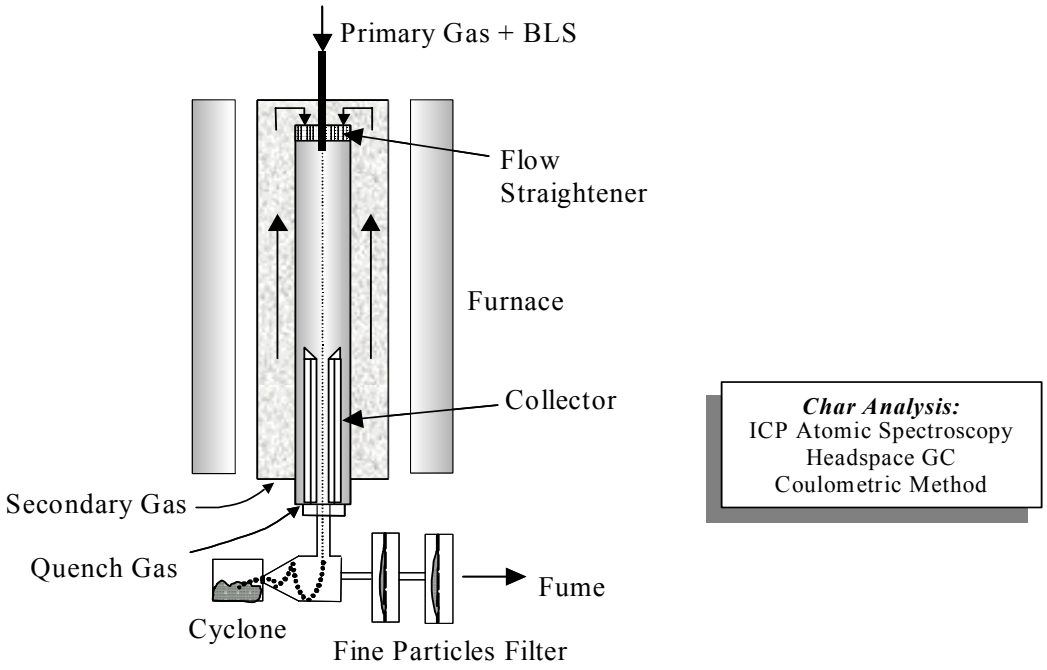

Figure 3.1: Schematic of the laminar entrained-flow reactor [64]

The BLS particles are fed to the LEFR by a feeding system consisting of a cylindrical fuel particle container (i.e., test tube) driven slowly upward by a small motor and screw drive:

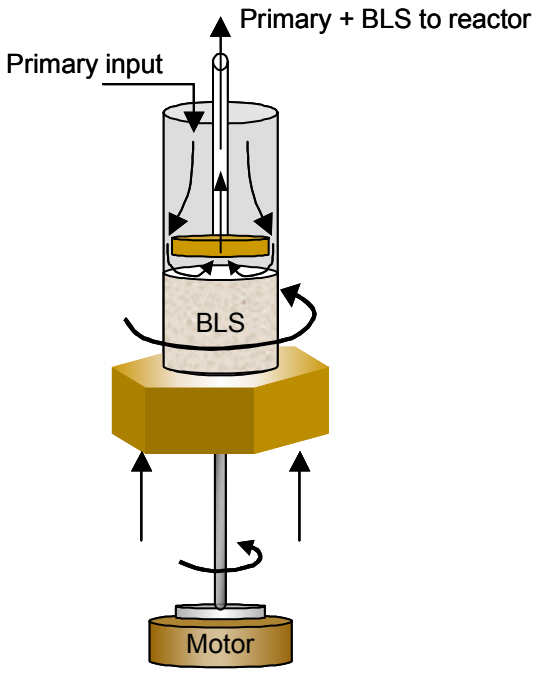

Figure 3.2: Black liquor solids feeding system [64]

A much smaller diameter feeding tube with a stationary plate is fixed in position coaxially inside the fuel particle container. A primary gas flow (pure N_2, flowing at 0.124 L/min and at room temperature during this work) enters the fuel particle container at the top and ventures through the feed tube. As the container moves upward, particles are removed from the surface of the solids and carried into the feeding tube by the gas. The feed rate of the particles is controlled by adjusting the upward displacement velocity of the fuel particle container relative to the stationary feed tube [62]. The feed rates in this work range from 0.025 to 0.045 g of BLS/min.

The LEFR consists of a reactor core – a cylindrical ceramic tube, 7 cm ID by 1 m length, inside a three-zone furnace with a total heated length of 0.83 m. The primary gas transfers black liquor particles from the feeder, via the small-diameter

feeding tube, into a water-cooled injector (3.3 mm ID) at the top of the reactor. A much larger, secondary gas flow (N_2, CO_2, and H_2O, 10 L/min at room temperature) enters the bottom of the reactor and is preheated to the desired reaction temperature as it passes through the reactor. The secondary gas makes a 180^o turn and then passes through a ceramic honeycomb flow straightener that is concentric with the primary gas and particle injector. The secondary gas passes through the flow straightener, and the resulting flow initially has a flat velocity profile that quickly develops into a laminar velocity profile. As the particles enter the reactor with the aid of the laminar primary gas flow, they are rapidly heated by convection and radiation, and as they flow downward, they remain in a narrow column along the center of the reactor.

After the desired residence time in the reactor, the reaction products are rapidly quenched in a water-cooled, nitrogen-purged collection system. This movable collector consists of a porous inner wall, through which pure, room-temperature nitrogen gas is passed to quench the reaction products and to terminate gasification reactions. At the exit of the collector, the product temperature had been reduced to 200-300^{o}C [64]. The gas and particles are separated at the bottom of the collector by a cyclone with a 3 μm particle cutoff, and as the gases and fume from gasification exit the system, the char residue remains. Particles larger than 3 μm in diameter are removed from the cyclone for char analysis, while the fine particles (fume) accumulate on a nylon membrane filter located upstream of the gas exhaust duct.

For all gasification experiments with the LEFR, the reactor was initially pre-heated with the secondary gas at the desired flow rate before activating the particle feeder and primary gas. The secondary gas mixture was created by first mixing pure

CO_2 and N_2 from separate gas cylinders and then passing the mixture through a steam generator, as shown in Figure 3.3:

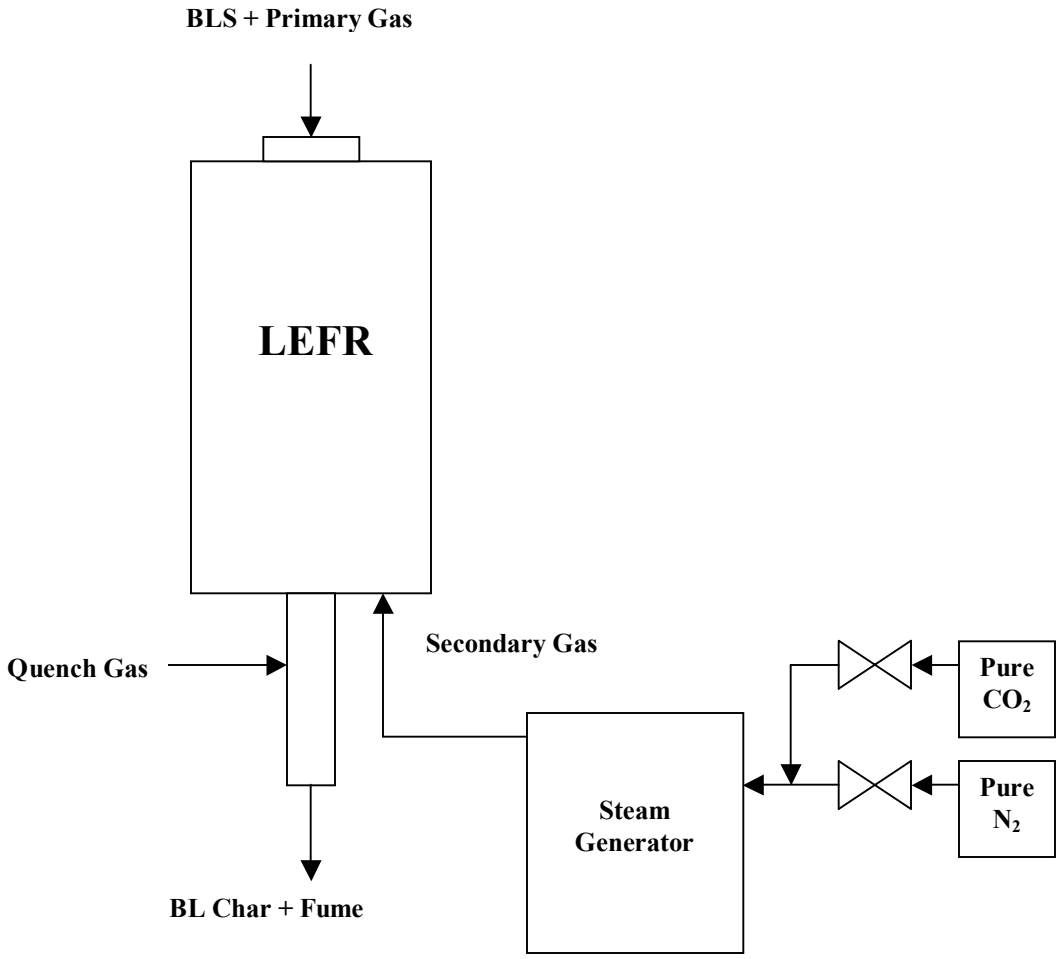

Figure 3.3: Use of a steam generator to produce secondary gas for the LEFR

The steam generator is essentially an electrically heated, insulated bubble column filled with water. The N_2/CO_2 secondary gas mixture enters the steam generator in the form of bubbles, and as the bubbles mix with the water, a saturated vapor forms. The concentration of H_2O in the saturated vapor is temperature-controlled, and to achieve a composition of 10% H_2O in the secondary gas, the steam

generator temperature was maintained at 50.3°C for all runs. This temperature was determined by a thermodynamic analysis of the secondary gas stream.

As the LEFR heated to the desired reaction temperature, the BLS, feeding tube, and the plate attached to the feeding tube were heated in an oven at 120°C for at least 2 hours to prevent moisture accumulation during the runs. The presence of moisture in the feeder and in the BLS led to injector plugging, which caused delays in experimentation. After drying, the feeder was prepared, and the secondary gas flow and steam generator were initiated. After a steady state was established, the particle feeder was activated so that the primary gas and BLS particles began to flow through the reactor. The duration of each experimental run ranged between 15 and 25 minutes, long enough to feed a sufficient amount of material into the reactor while preventing plugging problems.

At the completion of each run, the cyclone was removed from the collector and transferred to a nitrogen-purged glove bag that maintained an oxygen concentration of below 0.6% by volume. The char residue in the cyclone was weighed with a digital balance, and a portion (15-25 mg) was mixed with 1 mL de-ionized water and sealed in a 21.6 mL sample vial for char analysis. Meanwhile, the remainder of the char residue was saved in a sealed sample jar (I-Chem Series 300) for ionic species and total carbon analyses. The glove bag was necessary to prevent the extremely reactive char residue from oxidizing or combusting spontaneously upon exposure to air. Before resuming all LEFR runs, the injector was cleaned with a steel rod to dislodge accumulated particles, and the black liquor solids were briefly heated and screen sieved again to maintain dry particles in the desired size range. After every other run,

the cyclone was washed in de-ionized water and dried, and the feeding tube was cleaned with pure ethanol to dislodge accumulated solid particles.

3.4. The Use of Headspace Gas Chromatography in Char Analysis

An analysis method known as phase reaction conversion headspace gas chromatography (PRC-HS-GC), developed by Chai et al., was used to analyze the alkali carbonate content in the char [11-12]. This method is a type of flow-injection analysis (FIA) technique, as the sample is injected directly into the GC with the aid of a carrier gas. In the case of alkali carbonate, the GC measures the amount of carbon dioxide gas produced from the reaction of carbonate in the char sample matrix with sulfuric acid:

$$Na_2CO_3(s) + H_2SO_4(aq) \rightarrow Na_2SO_4(aq) + H_2O + CO_2(g) \qquad (3.1)$$

A 21.6 mL empty vial, sealed with a PTFE/butyl molded septum, was injected with 500 μL of 2 mol/L sulfuric acid. After the sulfuric acid was added, the GC measured the CO_2 content in the vial for a standard, or blank, concentration. The solid sample solution was prepared by dissolving 15-25 mg of char in 1 mL de-ionized water in a separate vial during the gasification runs. A microsyringe injected roughly 100 μL of this sample solution into the sealed vial to react with the sulfuric acid, and the CO_2 produced from the reaction was preserved in the vial.

The CO_2 measurements were carried out using an HP-7694 automatic headspace sampler and an HP-6890 capillary GC. The headspace sampler removes the CO_2 from the vial and transfers it along with a helium carrier gas to the GC, where

a thermal conductivity detector measures CO_2 concentrations. The GC and headspace sampler operating parameters for this work are summarized in Table 3.4:

Table 3.4: Operating parameters for the headspace-GC method [62]

GC Parameters	
Column	GS-Q capillary column, 30 m × 0.53 mm I.I
Detector	Thermal conductive detector (TCD)
Carrier gas	Helium at 3.1 mL/min
Oven temperature	30°C
Headspace Sampler Parameters	
Oven temperature	60°C
Vial equilibration time	0.5 min
Vial pressurization time	0.2 min
Sample-loop fill time	0.2 min
Loop fill time	1.0 min
Loop equilibration time	0.05 min

In each sample, the measured CO_2 concentration (i.e., the peak area for CO_2 in the chromatograms) was compared to the standard concentration to determine the true amount of CO_2 produced from the char. Using experimental correlations between carbonate concentration and the amount of CO_2 in the headspace, the concentration of carbonate in each sample was determined. The carbonate in the original black liquor solids was also analyzed in the same manner.

The reproducibility of this analysis technique is within ±0.15%, which is as good as coulometric or titrametric methods used by commercial laboratories. However, this method is much simpler, less time-consuming, and less costly than the coulometric and titrametric methods [59, 66]. Additionally, the headspace method

was also proven to surpass the reproducibility of traditional ion chromatography (IC) and capillary electrophoresis (CES) techniques [1, 6, 11-12].

The headspace GC method was also used to determine the amount of hydroxide produced from all alkali species in the char residue. The same principle holds for the hydroxide analysis: the solid char sample is acidified to produce a product gas that is detectable by the GC. In this analysis method, roughly 200 μL of the solid char sample solution was mixed with 200 μL of 1N HCl in a sealed sample vial. The HCl and char solution were then mixed vigorously in an ultrasonic vibrator for 3 min at 60°C. During the mixing, 500 μL of 1N $NaHCO_3$ buffer solution was added to an empty vial, which was then analyzed by the GC to determine the standard CO_2 concentration. After the standard measurement was made, roughly 200 μL of the HCl-char sample solution was injected by a microsyringe into this vial.

The overall, simplified reaction that occurs during the analysis is as follows:

$$CharSample + H_2O + HCl(aq) + NaHCO_3(aq) \rightarrow CO_2(g) + NaCl(aq) \qquad (3.2)$$

To accomplish complete reaction, HCl and $NaHCO_3$ solutions were added in excess. Using the same operating conditions listed in Table 3.4, the GC measured the concentration of CO_2 produced in the headspace, and using experimental correlations, the amount of hydroxide produced from the char sample was determined. Like the carbonate method, the peak CO_2 areas for the samples were compared to the peak CO_2 areas for the standard solutions, and the difference between these peak areas yielded the true amount of CO_2 produced by the char. The reproducibility of this technique is within ±0.15%, which is superior to the titrametric hydroxide analysis methods used

by commercial laboratories [59]. Additionally, this method is simpler (i.e., requiring much smaller sample sizes) and less time-consuming than titrametric methods, and it is comparable to other analytical methods encountered in the literature [70].

3.5. Analysis of Ionic Species, Total Carbon, and Char Yields

While a portion of the char residue was placed in a sealed vial for analysis with the headspace GC method, the remainder of the char residue was placed in a sample jar (I-Chem Series 300) for ionic species and total carbon analyses. The Chemical Analysis Group of the Institute of Paper Science and Technology conducted these analyses, and the results were useful in furthering the understanding of chemical species transformations during gasification conditions. Moreover, the results allowed for a more accurate method of determining char yields for each experimental run.

The Chemical Analysis Group measured the amounts of alkali metals (Na and K), sulfur, and calcium using a method known as inductively coupled plasma atomic emission spectroscopy (ICP-AES). This method is based on the principle that during the return to the ground state, an excited atom or ion releases absorbed energy as light (photons) of characteristic wavelengths, the positions and intensities of which can be measured [8, 59]. The energy transfer for electrons after falling back to the ground state is unique to each element, as it depends upon the electronic configuration of the orbitals. Because the energy transfer is inversely proportional to the wavelength of electromagnetic radiation, the wavelength of light emitted is also unique.

The Chemical Analysis Group uses the Perkin Elmer Optima DV3000 for all ICP-AES analyses. In this device, the plasma (ionized argon gas in this case) is generated from radio frequency (27.12 Hz) magnetic fields induced by a copper coil,

which is wound around the top of a quartz torch. The high frequency current flows in the coil generating a rapidly varying magnetic field within it. The ionic particles of the plasma flow through the magnetic field and cause a flame through which the sample passes. As the sample is injected into the plasma, it heats up rapidly and produces atomic emission lines that can be detected by an analyzer. The analyzer quantifies the emission lines from each element, and from this information, it computes the concentrations of each element in the sample. The device uses 50-200 mg of material for each sample, and the reproducibility ranges between ±5% and ±20% [8]. The sample must be homogeneous for accurate measurements, and black liquor char is sufficiently homogeneous for this analysis [49, 63].

The Chemical Analysis Group measured the total carbon content in the char by using the so-called coulometric method. Basically, this method uses electrolysis, and the amount of electrical charge (in units of coulombs) used to release elemental carbon from the sample is related to the total amount of carbon originally in the sample [59]. The reproducibility of this technique is within ±5%. While the results for the coulometric method are not as precise as the headspace GC method, the use of this method internally was far more convenient than sending the samples to external laboratories for analysis. The short timeframe associated with on-site analyses also produced more accurate results because changes in chemical composition occur in the highly reactive black liquor char over time.

The ICP-AES method analyzed the calcium content of both the black liquor solids and the char residue. While the amount of calcium is quite small relative to alkali and carbon species in both black liquor solids and char (less than 0.1 wt. % in

both black liquor solids and char), it is very useful in accurately calculating the char yield during gasification experiments. The calcium material balance between the solids and the char is as follows:

$$M_{BLS} \cdot X_{Ca\_BLS} = M_{Char} \cdot X_{Ca\_Char} \qquad (3.3)$$

In Equation 3.3, X_{Ca_BLS} represents the concentration of calcium in BLS, X_{Ca_Char} represents the concentration of calcium in the char, M_{BLS} represents the total mass of BLS fed to the LEFR, and M_{Char} represents the mass of char residue. The char yield is defined as the ratio of the mass of black liquor char to the amount of black liquor solids fed to the reactor, and assuming that calcium does not vaporize (bp = 1484^{o}C), the char yield is determined by the following equation:

$$CharYield = M_{Char} / M_{BLS} = X_{Ca\_BLS} / X_{Ca\_Char} \qquad (3.4)$$

Because of plugging and agglomeration of solids in the injector of the LEFR, the actual ratio of masses does not yield an accurate representation of the mass loss that occurs during devolatization and gasification, and this leads to inaccurate char yields. However, if calcium does not vaporize, it passes through the entire reaction path of the LEFR in the char phase, and as a result, the ratio of calcium concentrations yields accurate char yields.

CHAPTER 4

RESULTS AND DISCUSSION

4.1. Char Residue Yield Analysis

As mentioned in Chapter 3, the measurement of calcium concentrations in the BLS and in the char residue enabled determination of accurate char yields during the gasification experiments. Because calcium does not vaporize during the gasification conditions in this work, it remains entirely in the condensed phase through the entire reaction path of the LEFR and can be used as a tie element to correct char yield data when not all of the char is collected. Figure 4.1 shows the char yields of all gasification runs:

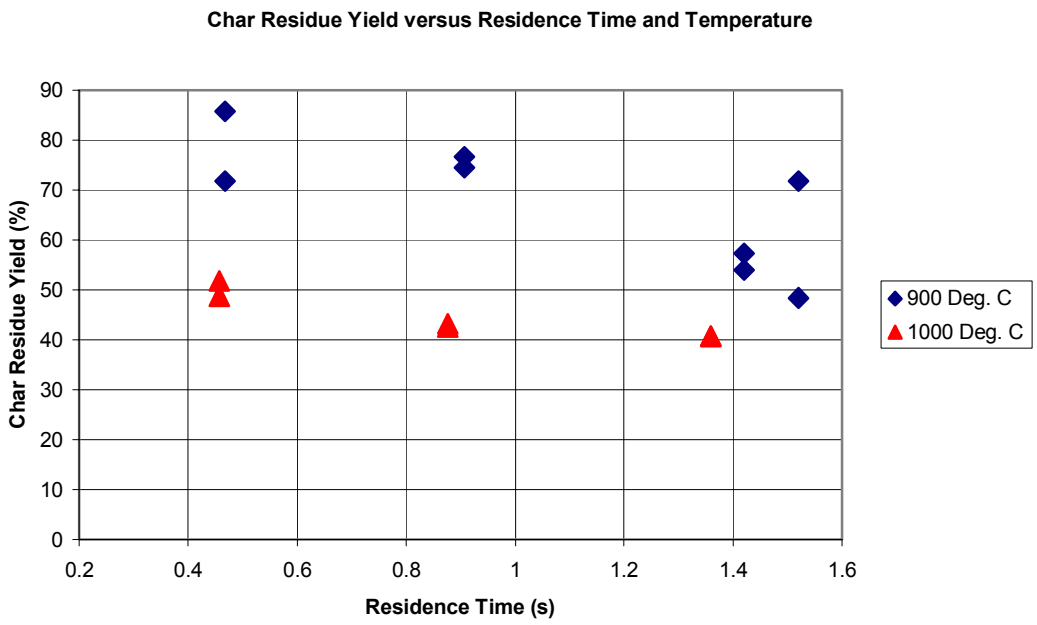

Figure 4.1: Char residue yields from the gasification runs

Devolatilization occurs very rapidly starting at temperatures above 200°C, and the results in Figure 4.1 are consistent with the fact that devolatilization is

essentially complete as soon as heat is transferred to the BLS particles. The loss of volatile gases and significant mass losses due to pyrolytic decomposition occur in less than 0.3s at 900-1000^{o}C, with higher losses (i.e., up to 50%) occurring at 1000^{o}C [31, 66, 67]. The majority of the mass loss at 900^{o}C and 1000^{o}C in this work occurs with devolatilization even before the earliest residence times studied. Further mass loss (i.e., via inorganic sulfate reduction processes in Eq. 2.9 and 2.10 and carbonate destruction in Eq. 2.18) occurs at lower rates at longer residence times and, therefore, at higher carbon conversions.

Given experimental uncertainty, the presence of H_2O and CO_2 gasifying agents during high-temperature conditions does not appear to have a significant impact on char residue yields, as compared to using one gasifying agent or pyrolysis conditions. In the work of Sricharoenchaikul, gasification with water vapor concentrations of 12% and gasification with CO_2 concentrations of 5% yielded comparable char yields at both 900^{o}C and 1000^{o}C. However, given experimental error in char yield measurements, the gasifying agents did not significantly impact char yields compared to pyrolysis conditions [62, 66-67]. In this work, the highest measured char yields are slightly higher at 900^{o}C (86% at 0.5 s) and slightly lower at 1000^{o}C (49% and 52% at 0.5 s) than those in the work of Sricharoenchaikul. On the other hand, the lowest measured char yields (48% at 1.5 s and 900^{o}C, and 41% at 1.4 s and 1000^{o}C) are still comparable to the lowest measured char yields obtained with one gasifying agent or pyrolysis conditions.

Despite apparently erroneous char yields (72% at 0.5 s, and 72% at 1.5 s) due to errors in the ICP-AES calcium analysis, the lack of significant changes in char

yields for both pyrolysis and gasification conditions may be due to the adsorption of CO_2 and H_2O to the catalytic activation sites in the char. CO_2 chemisorbs strongly to the catalytic sites within the char and stabilizes them along with H_2O, and this results in an increase in apparent char mass. The increase in apparent char mass may be significant enough to cause artificial similarities in char yields between pyrolysis and gasification conditions [55].

4.2. Analysis of Carbonate Content in the Char

The content of alkali carbonate in the char is shown below in two ways. Figure 4.2 shows the concentration of alkali carbonate in the char as determined by the headspace GC method. It was assumed that the alkali carbonate was all Na_2CO_3, since sodium accounts for 95-96% of the alkali metals in the char. Figure 4.3 shows the fraction of total liquor carbon as carbonate carbon, which is the amount of carbon in the char in the form of alkali carbonate species relative to the amount of total carbon fed to the LEFR:

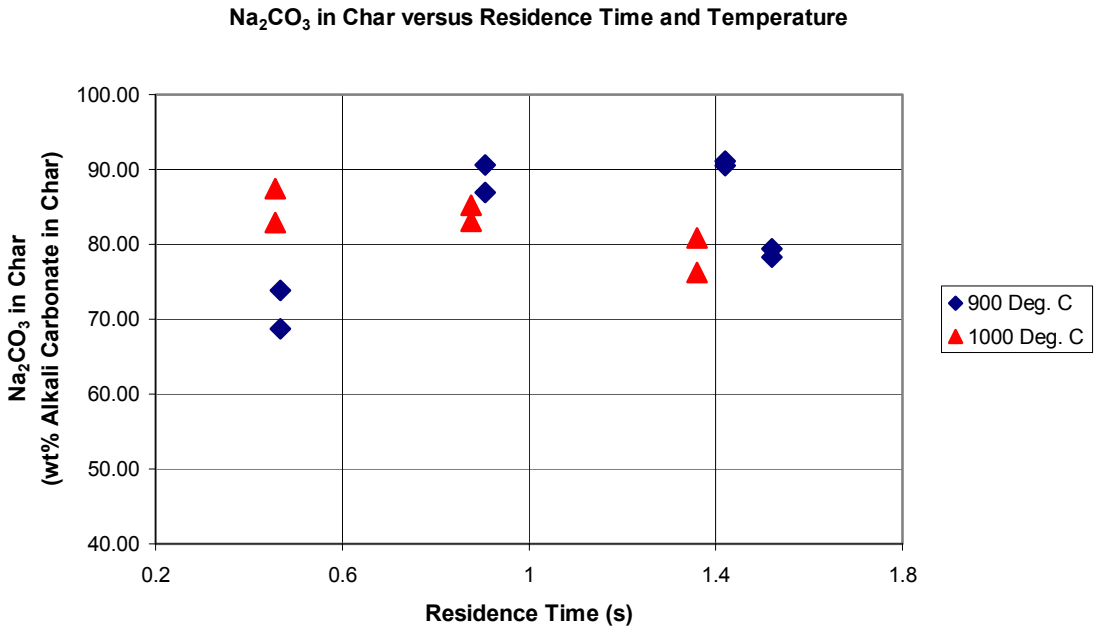

Figure 4.2: Weight percent of Na_2CO_3 present in the char from carbonate measurements

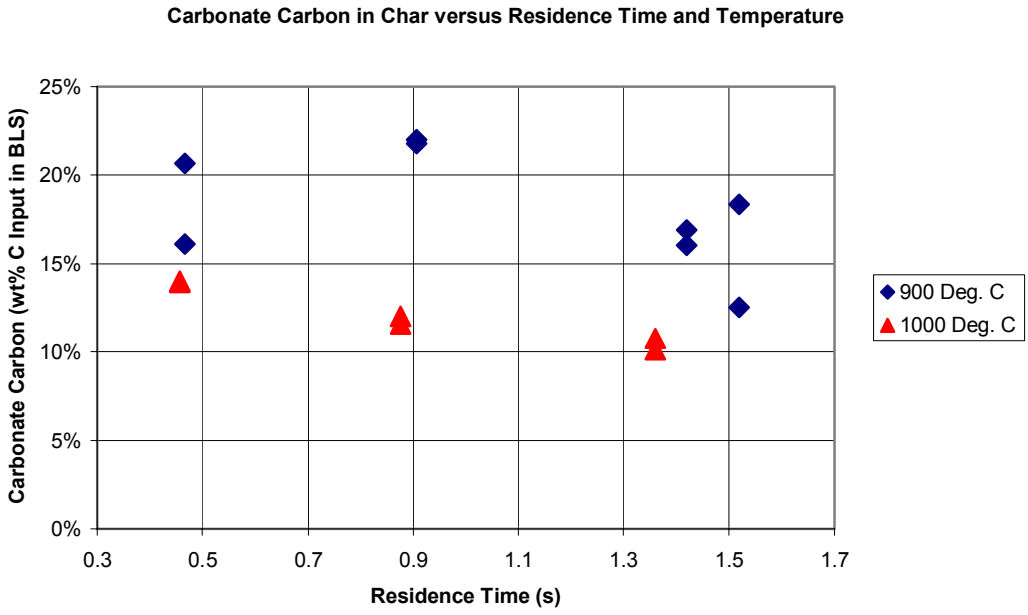

Figure 4.3: Carbonate carbon in black liquor char, relative to carbon input in the BLS

The fraction of liquor carbon as carbonate carbon originally in the BLS before gasification was 3.3%. Previous work has shown that very little carbonate is formed relative to the initial amount occurs at low-temperature conditions at short residence times, yet during high-temperature conditions, significant changes in carbonate carbon content occur. The results in Figure 4.3, disregarding the apparently erroneous data points of 21% at 0.5 s and 18% at 1.5 s, are consistent with theory discussed in Chapter 2 of this thesis. At 900°C, the carbonate carbon increases rapidly, and then at longer residence times, the carbonate decreases. This implies that carbonate formation is initially more rapid than carbonate decomposition, but then later, carbonate decomposition becomes dominant, thus reducing carbonate carbon.

Previous work has shown that a combination of H_2O and CO_2 increases the formation of carbonate via Equation 2.13. In the presence of only CO_2, the maximum carbonate carbon produced was 14% of the carbon input, and in the presence of 5% H_2O and 12% H_2O, the carbonate carbon reached a maximum of 16% [66]. In this work, the maximum carbonate carbon is almost 22% of the carbon input at a residence time of 0.9 s, which may indicate that prior to carbonate destruction, the presence of two oxidizing agents is significantly more effective in producing carbonate. At 1000°C, the data in Figures 4.2 and 4.3 suggest that carbonate formation at early residence times is reduced due to higher carbon oxidation rates, and carbonate destruction occurs at a higher rate at later residence times in this work. However, the carbonate destruction is not as severe, particularly at 1000°C, as it is for pyrolysis conditions because the oxidizing agents stabilize catalytic sites (i.e., preventing

reduction of the carboxylate and phenolate moieties to unstable alkali carbide species) in the char [33, 66].

4.3. Analysis of Fixed Carbon and Total Carbon in the Char

Figures 4.4 and 4.5 show the effects of temperature and residence time on total carbon and fixed carbon (both of which are relative to the initial carbon input) in the char:

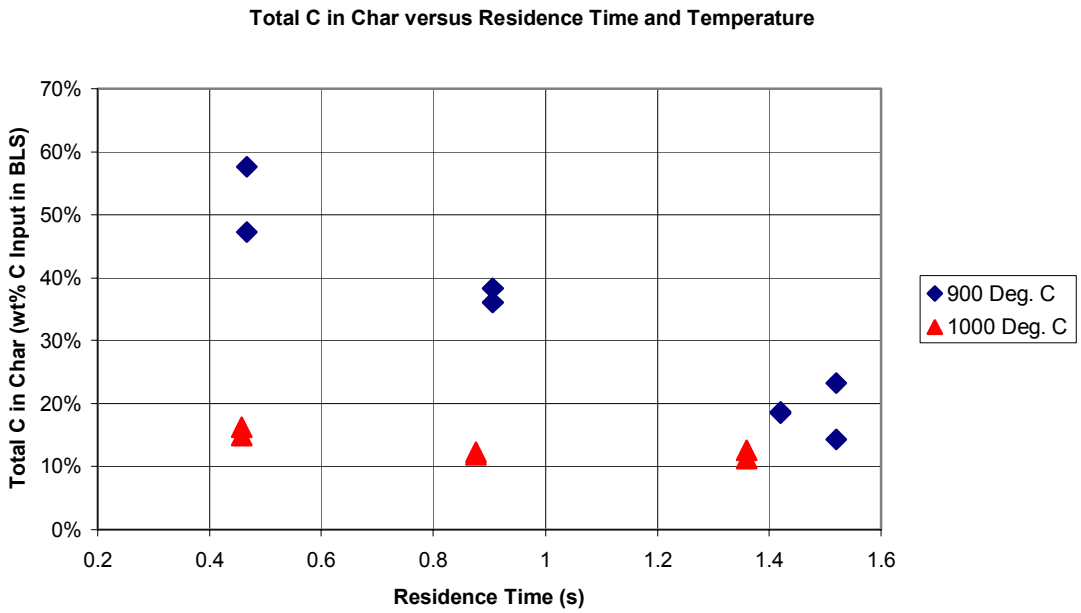

Figure 4.4: Total carbon in black liquor char, relative to carbon input in BLS

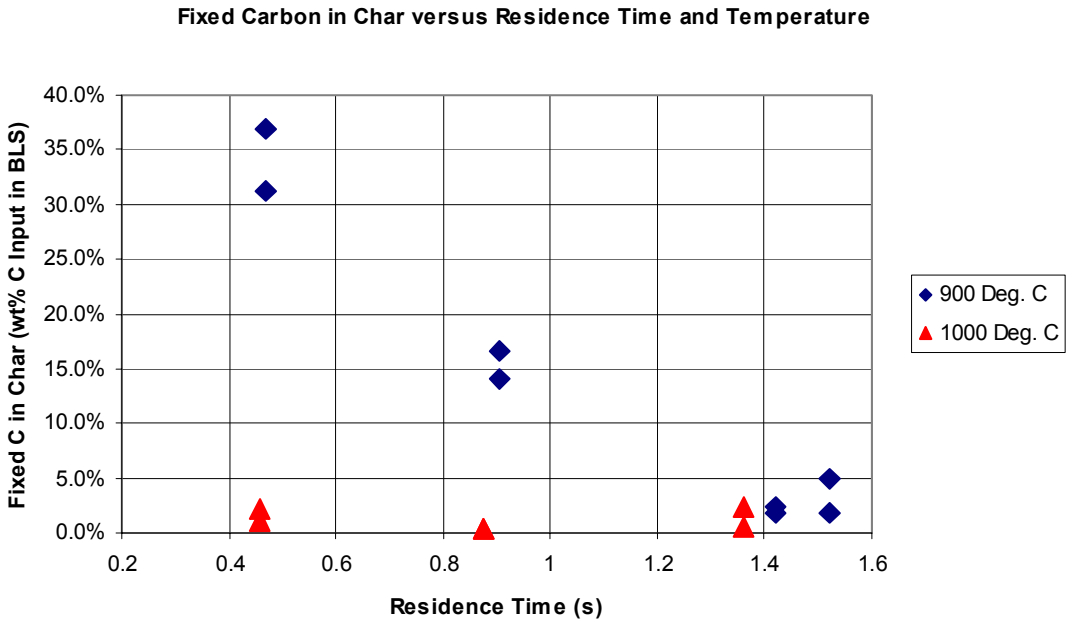

Figure 4.5: Fixed carbon in black liquor char, relative to carbon input in BLS

The fixed carbon in the char was calculated by taking the difference between the total carbon, as determined by the coulometric method, and the carbonate carbon. The initial amount of non-carbonate carbon in the BLS was 96.7% of the total carbon, and at 900°C and 1000°C, both the non-carbonate carbon and total carbon decreased tremendously. The presence of both H_2O and CO_2 apparently enhances gasification rates relative to gasification with a single oxidizing agent or pyrolysis conditions, and this may have caused the fixed carbon and total carbon levels to be significantly lower than those measured in previous studies [66].

In the work of Sricharoenchaikul, as much as 63% of the fixed carbon was converted to volatile species within the shortest residence times at 1000°C during pyrolysis or gasification with either CO_2 or H_2O, whereas in this work, as much as 95% of the fixed carbon is converted to volatile species by the earliest residence times at the same temperature. Essentially all of the fixed carbon was converted at an

intermediate residence time at 1000°C, whereas essentially all of the fixed carbon was converted at later residence times in the presence of one oxidizing agent. Additionally, the presence of H_2O and CO_2 resulted in substantially higher conversions of total carbon at 1000°C, with total carbon conversions being as much as 35% higher at the earliest residence time compared to pyrolysis and gasification with one oxidizing agent. The results in this work suggest that the presence of two oxidizing agents may greatly enhance the conversion of carbon in BLS to light gases, condensable organic matter, and tars even at the shortest residence times studied.

4.4. Retention of Alkali Metals and Sulfur in the Char

The retention of alkali metals and sulfur in the char was studied to solidify the understanding of carbon species transformations during gasification. Figure 4.6 shows the retention of sodium in the char, and Figure 4.7 shows the retention of potassium in the char:

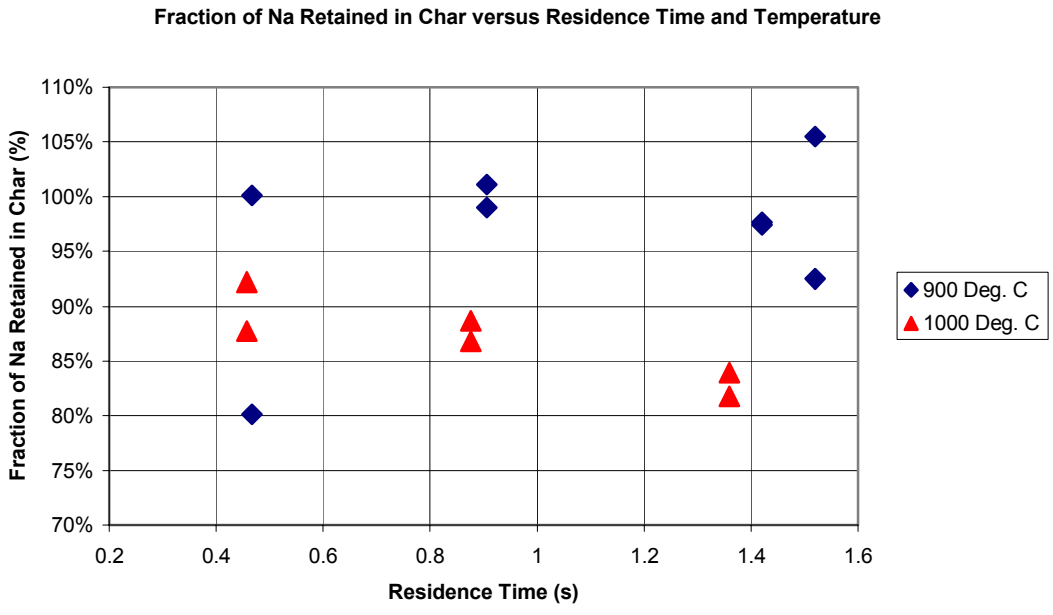

Figure 4.6: Sodium retention in the char during gasification

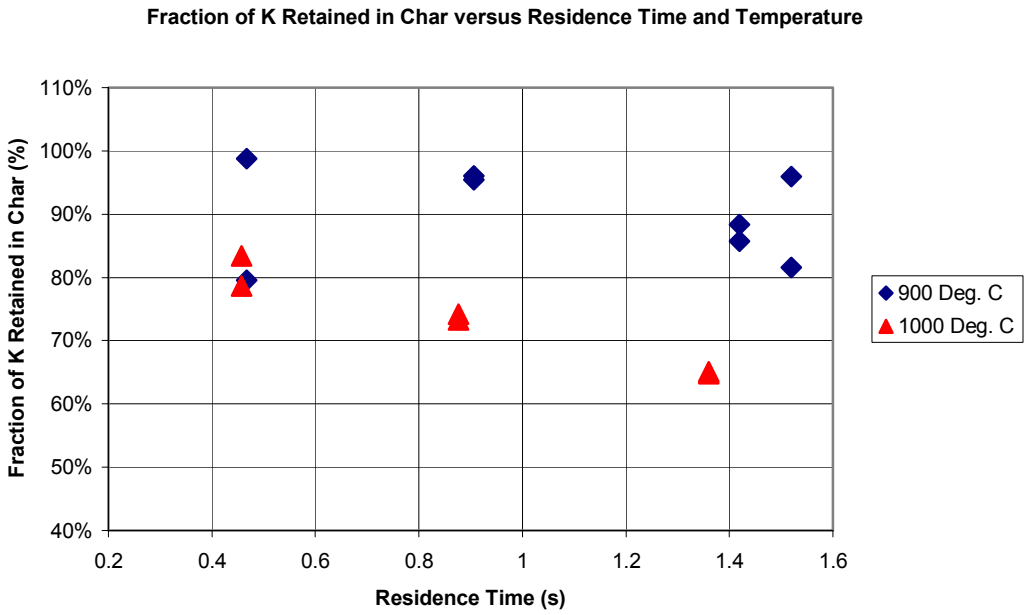

Figure 4.7: Potassium retention in the char during gasification

The 105% sodium retention and 96% potassium retention at the last residence time, and the 80% sodium and potassium retentions at the earliest residence time are deemed erroneous due to errors in the char residue analysis. Overall, the results shown in Figure 4.6 suggest that in the presence of H_2O and CO_2 oxidizing agents, sodium does not vaporize until later residence times at 900^{o}C, and the amount of sodium vapor produced is not as large as that produced during pyrolysis. This is consistent with the idea that alkali metal vapor formation is suppressed in the presence of oxidizing agents [33, 58, 63, 66]. The lower levels of alkali metal volatilization correspond to lower rates of carbonate destruction and higher stability of char catalytic sites, which occurs in the presence of oxidizing agents. At 1000^{o}C, on the other hand, carbonate decomposition processes are more dominant overall, which means that the catalytic sites in the char are less stable overall and produce higher amounts of alkali metal vapors, which is seen in Figures 4.6 and 4.7. As the alkali metals enter the

product gas, less alkali metal species associate with carbonate species, and this results in lower levels of carbonate in the char. Potassium volatilization occurs more easily at both 900°C and 1000°C and at all residence times due to the fact that potassium salts are more volatile, but the volatilization occurs in the same manner as it does for sodium [13-14, 33, 58, 72].

The overall fraction of sulfur retained in the char with respect to temperature and residence time during the gasification runs is shown as follows:

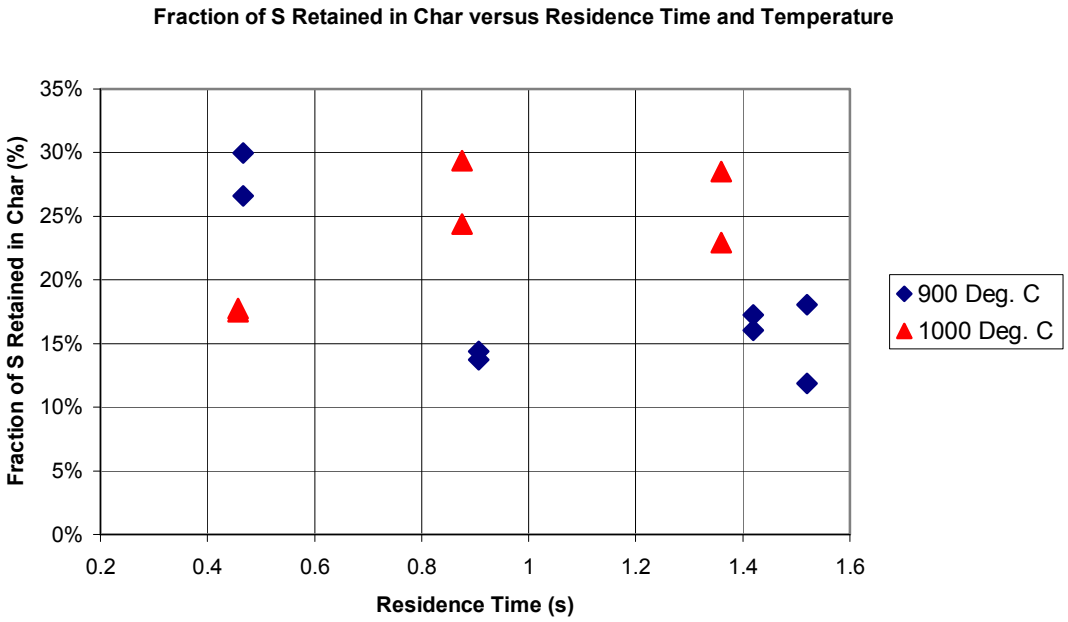

Figure 4.8: Sulfur retention in the char during gasification

As mentioned in Chapters 1 and 2, one important feature of gasification is the natural split between alkali species and sulfur species. In gasifiers, the majority of the sulfur species is converted to gases while the majority of the alkali species are retained in the char. This observation is apparent in Figures 4.6-4.8, as the amount of sulfur species retained in the char is significantly lower than the retained amount of alkali metals. The higher final sulfur retention at 1000°C than at 900°C is consistent with the

fact that conditions are thermodynamically favorable for greater sulfur levels in the char at higher temperatures. In other words, sulfur capture is an exothermic process. This corresponds to the fact that higher splits between alkali metals and sulfur occur during low-temperature gasification processes than during high-temperature gasification processes.

4.5. Hydroxide Formation in Black Liquor Char

Figure 4.9 shows the amount of alkali as hydroxide divided by the amount of alkali species as hydroxide and carbonate for all gasification conditions in this work.

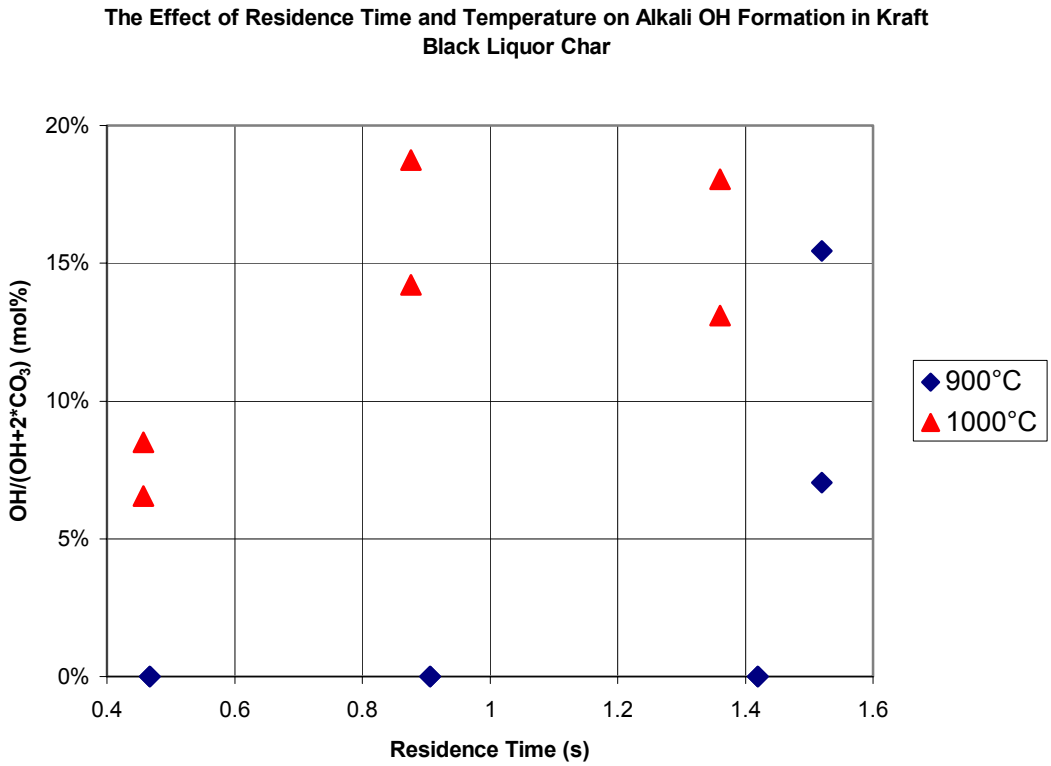

Figure 4.9: Hydroxide formation in the char versus residence time and temperature

The hydroxide formation data suggest that at 900°C, no significant amounts of hydroxide are produced until after 1.4 s, but at 1000°C, hydroxide appears to form readily even at the earliest residence times studied. The char produces a maximum mole percent of 18-19% hydroxide in this work, starting at intermediate residence times at 1000°C. Figure 4.10 shows the relationship between hydroxide formation and the levels of carbonate carbon at 1000°C, and Figure 4.11 shows the relationship between hydroxide formation and fixed carbon at both 900°C and 1000°C:

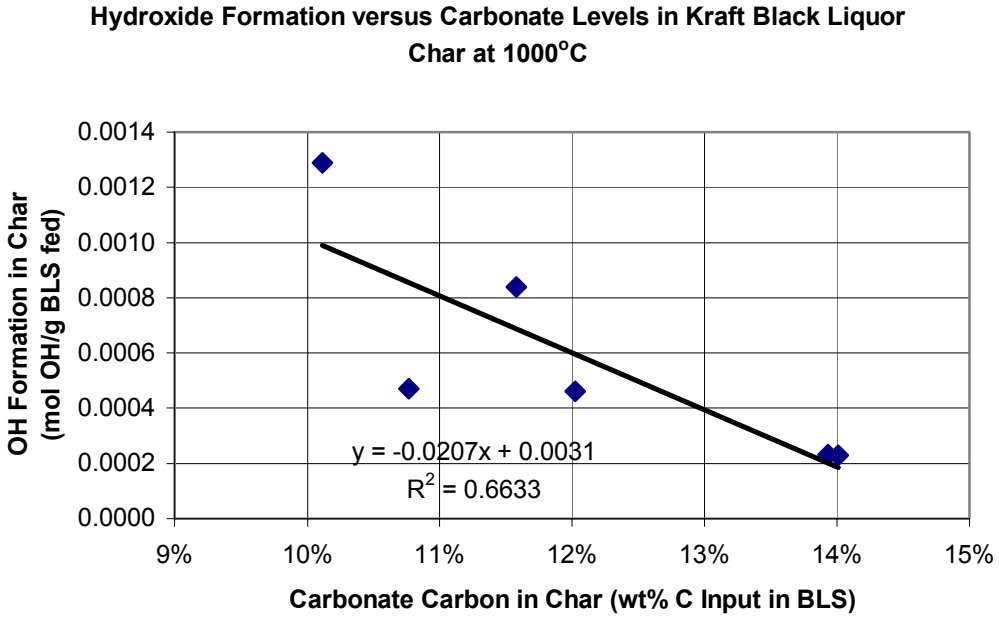

Figure 4.10: Relationship between OH formation and carbonate carbon at 1000°C

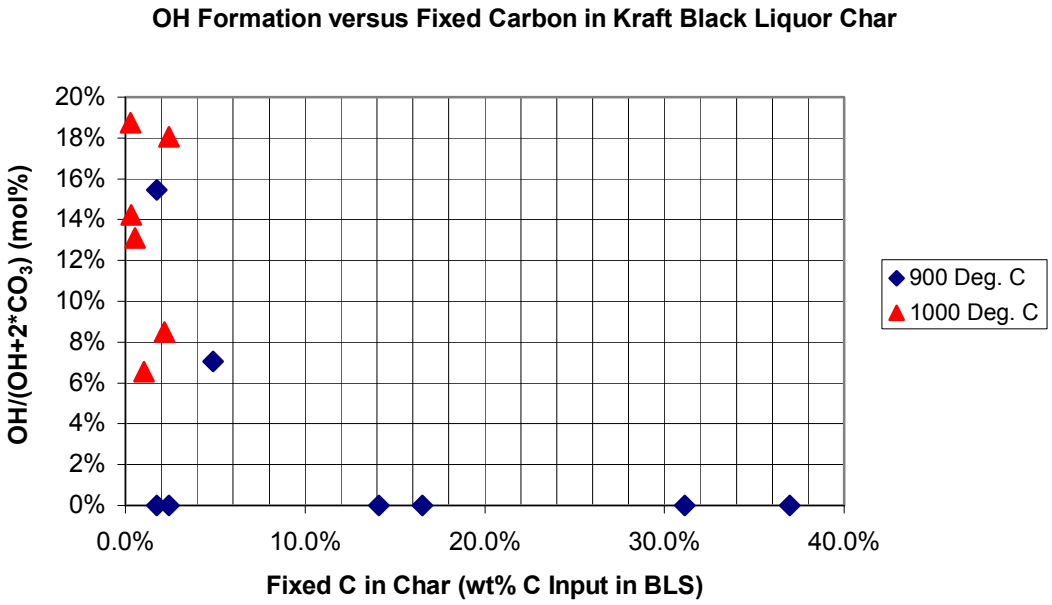

Figure 4.11: OH formation versus fixed carbon in char

In this work, significant amounts of hydroxide are not produced until at least 95% of the original fixed carbon in black liquor is consumed during gasification. In the presence of H_2O and CO_2 gasifying agents, a 95% fixed carbon conversion occurs at the earliest residence times at 1000°C. At 900°C, the carbon oxidation rates are apparently lower than at 1000°C, which means that a 95% fixed carbon conversion does not occur until after 1.4 s, at which point measurable amounts of hydroxide are formed. The results in Figure 4.11 suggest that significant hydroxide formation does not occur until the fixed carbon conversion is almost complete.

Figure 4.10 suggests that at 1000°C, a weak inverse linear correlation (r^2 = 0.66) exists between the amount of hydroxide produced (relative to the amount of black liquor solids fed to the reactor) and the amount of carbonate carbon in the char. At 900°C, a correlation does not exist, as hydroxide is not formed until after a 1.4 s

residence time. At this point, the fixed carbon conversion is at least 95% at both 900°C and 1000°C. The data suggest that hydroxide formation may not occur until carbonate destruction processes begin to dominate, and these processes do not dominate until high fixed carbon conversions occur.

The trends observed in Figures 4.10 and 4.11 can be explained in terms of the interactions of the organic catalytic moieties in the char. The main catalytic species in black liquor char residue are in the form of phenolate and carboxylate functional groups, which remain stable in the presence of oxidizing agents. However, later in the gasification process, fixed carbon becomes depleted, and the moieties form alkali carbonate species.

The specific interaction of the moieties may be explained by the following reaction mechanisms involving both H_2O and CO_2 oxidizing agents:

$$C-O-Na+H_2O \rightarrow Na-O-C=O+H_2 \quad (4.1)$$

$$Na-O-C=O+C \rightarrow C-O-Na+CO \quad (4.2)$$

$$C+H_2O \rightarrow H_2+CO \quad (4.3)$$

$$C-O-Na+C \rightarrow C-Na+CO \quad (4.4)$$

$$C-Na+CO_2 \rightarrow C-O-Na+CO \quad (4.5)$$

$$C+CO_2 \rightarrow 2CO \quad (4.6)$$

Both mechanisms involve the moieties and gasifying agents and as seen in Equations 4.3 and 4.6, they also yield the overall carbon gasification reactions with H_2O and CO_2. They also correspond to the general reaction mechanisms shown in Equations 2.3-2.6. In the H_2O gasification mechanism, the phenolate moieties (C-O-Na) originally in the char react with adsorbed H_2O to form a carboxylate group (Na-O-

C=O), which then reacts with an adjacent free carbon site to re-generate phenolate moieties. In the CO_2 gasification mechanism, the phenolate moieties react with an adjacent free carbon site to form the alkali carbide species, while alkali carbide species react with CO_2 to re-generate phenolate moieties.

At 900°C, the fixed carbon conversion does not reach 95% until after a 1.4 s residence time, and prior to this residence time, no hydroxide is formed. However, at 1000°C, carbon conversion is almost complete at the earliest residence time studied and significant amounts of hydroxide are produced. This behavior suggests that significant amounts of phenolate moieties, which are converted directly to hydroxide upon dissolution in water, may not be present until the conditions are suitable for near-complete fixed carbon conversion. The carboxylate moieties do not form hydroxide upon dissolution in water, but rather form aqueous carbonate species. At 1000°C, the carbon gasification rates in Equations 4.3 and 4.6 are apparently higher than at 900°C, which results in significant increases in reaction rates in Equations 4.2 and 4.4. The significant increase in hydroxide at 1000°C suggests that the rate of reaction in Equation 4.5 may be higher as well, which results in a significant amount of phenolate moieties remaining in the char for hydroxide production.

The reaction mechanisms shown in Equations 4.1-4.6 are apparently consistent with the overall framework for the interaction of moieties and formation and destruction of carbonate in Chapter 2. At 1000°C, carbonate destruction processes become dominant along with higher carbon gasification rates, and more alkali metal vapors are formed at this temperature than at 900°C. This suggests that while the gasification processes increase the amount of phenolate moieties in the char residue,

the rate of alkali carbide species formation increases as well, and these species become unstable and produce alkali metal vapors. While more alkali metals enter the gas phase and carbonate is reduced, more phenolate moieties are available in the remaining char to form hydroxide. At 900°C, carbonate formation processes appear to be favorable at early residence times, which is consistent with the observation that no hydroxide formation occurs until after a 1.4 s residence time. At this temperature, the moieties that have not been converted to carbonate may be mainly carboxylate moieties due to the high rate of Equation 4.1, but after 1.4 s, carbonate destruction and alkali metal formation processes occur, leaving phenolate moieties in the char for hydroxide formation.

It is possible that sulfur speciation in the char residue may also play a significant role in hydroxide formation. Figure 4.8 shows the exothermic process of sulfur capture: as temperature increases, the final amount of sulfur retained in the char increases. At 900°C, the amount of sulfur reaches a minimum level and then after 1.4 s, the sulfur content apparently increases. Sulfide species produce hydroxide upon hydrolysis, but the experimental analysis revealed that very little sulfide remained in the char to form significant amounts of hydroxide. Therefore, sulfate species and other sulfur species, such as sulfite, could contribute to hydroxide formation in addition to the phenolate moieties. Additional studies of sulfur species transformations in black liquor char must be conducted to determine their role, if any, in hydroxide formation.

CHAPTER 5

CONCLUSIONS AND RECOMMENDATIONS

5.1. Conclusions

The work in this thesis focuses on the effects of high-temperature black liquor gasification with H_2O and CO_2 on hydroxide formation and the distribution of carbon species within the char product. The key measured dependent variables of the work are char yield, carbonate carbon within the char, alkali metal retention, sulfur retention, and hydroxide formation.

The presence of both H_2O and CO_2 appears to enhance carbon gasification rates, with carbon conversions of at least 95% at the earliest residence time at 1000^{o}C. The presence of both gasifying agents causes an increase in carbonate formation at early residence times at 900^{o}C, resulting in as much as 22% of the initial carbon input in the form of carbonate relative to as much as 16% with one gasifying agent. However, at residence times above 1.4 s at 900^{o}C and at all residence times at 1000^{o}C, carbonate destruction processes are faster than carbonate formation processes, which causes lower carbonate levels in the char. The retention of alkali metal species is high until carbonate destruction mechanisms become important, at which point alkali metal volatilization occurs. The retention of sulfur species is higher at 1000^{o}C than at 900^{o}C due to its exothermic behavior, and at 900^{o}C, the sulfur content appears to reach a minimum and then increases again at residence times beyond 1.4 s.

At 900^{o}C, no significant amounts of hydroxide are produced until after 1.4 s, but at 1000^{o}C, hydroxide appears to form readily even at the earliest residence times

studied. The char produces a maximum mole percent of 18-19% hydroxide in this work, starting at intermediate residence times at 1000°C. The formation of hydroxide may be explained by the interactions of organic catalytic moieties in the char; as conditions are suitable for greater phenolate species formation, more hydroxide can be produced. The results suggest that the formation of hydroxide is favorable at fixed carbon conversions of 95% and beyond, and at carbonate carbon levels of 15% of the initial carbon input. Both conditions are satisfied at all residence times at 1000°C, leading to the high levels of hydroxide formation at that temperature.

The hydroxide formation data suggest that it may be possible to develop an alternative causticization process that produces partial causticizing. With at least an intermediate residence time and operating temperatures of 1000°C, significant amounts of hydroxide can be produced without the addition of a decarbonizing agent. A one-stage process could be feasible, but additional studies must be done to determine if it is feasible.

5.2. Recommendations

While this work suggests that significant amounts of hydroxide can be produced with gasification in the presence of H_2O and CO_2, it would be interesting to study the impact of pyrolysis conditions on hydroxide formation. Pyrolysis conditions impact the interaction of catalytic moieties and carbonate formation processes differently within black liquor char, and having hydroxide formation data for pyrolysis conditions could offer interesting comparisons to hydroxide formation during gasification.

Additionally, a more thorough analysis of sulfur species transformations must be done to determine if sulfur speciation within the char has an impact, if at all, on hydroxide formation. Thorough sulfur species studies have been done for pyrolysis conditions, but few sulfur species studies have been done for gasification conditions, particularly for gasification with H_2O and CO_2. While the total amount of sulfur species retained in the char increases at high temperatures, the impact of sulfur species on hydroxide formation cannot be determined for certain in this work. A more complete profile of the fate of sulfide, sulfate, thiosulfate, and sulfite species in the char would be helpful in determining if other inorganic processes, in addition to the interaction of catalytic moieties, could produce hydroxide.

Finally, it would be interesting to repeat some of the experiments in this work with a different black liquor to determine if the elemental composition of the liquor can make significant differences on the output parameters. It would be helpful to determine with statistical confidence if subtle changes in elemental composition actually do have a significant impact on parameters, such as carbonate formation, hydroxide formation, and sulfur species transformations. Studying the effects of pressure on gasification conditions could allow for a more thorough fundamental understanding of the kinetic behavior of black liquor gasification and hydroxide formation during pressurized conditions. This information could provide more valuable insights into the practical aspects of gasification-causticization processes without the use of additional chemicals.

APPENDIX A

GASIFICATION RUN DATA

Table A1: Gasification run data – Runs 1-4

Run #	1	2	3	4
Sample ID	M04/12/05(1)	M04/13/05(1)	M04/15/05(1)	M04/15/05(11)
Feeding Material	BL	BL	BL	BL
Particle Size (mm)	90 - 125	90 - 125	90 - 125	90 - 125
Residence Time (s)	1.52	1.52	0.467	0.467
Temp. (^{o}C)	900	900	900	900
N_2 (%)	80	80	80	80
CO_2 (%)	10	10	10	10
Steam (%)	10	10	10	10
Primary flow (ml/min)	124	124	124	124
Seconday flow (L/min)	10	10	10	10
Quench flow (L/min)	10	10	10	10
Feeding Amount (g)	0.6105	0.7523	0.4491	0.5553
Feeding Time (min)	18	19	18	16
Feeding Rate (g/min)	0.034	0.040	0.025	0.035
Char Amount (g)	0.2516	0.1217	0.2110	0.1815
Char Yield (%)	41%	16%	47%	33%

Table A2: Gasification run data – Runs 5-8

Run #	5	6	7	8
Sample ID	M04/19/05(1)	M04/19/05(11)	M04/21/05(1)	M04/21/05(11)
Feeding Material	BL	BL	BL	BL
Particle Size (mm)	90 - 125	90 - 125	90 - 125	90 - 125
Residence Time (s)	0.906	0.906	1.42	1.42
Temp. (^{o}C)	900	900	900	900
N_2 (%)	80	80	80	80
CO_2 (%)	10	10	10	10
Steam (%)	10	10	10	10
Primary flow (ml/min)	124	124	124	124
Seconday flow (L/min)	10	10	10	10
Quench flow (L/min)	10	10	10	10
Feeding Amount (g)	0.5908	0.5962	0.8141	0.5204
Feeding Time (min)	17	15	18	18
Feeding Rate (g/min)	0.035	0.040	0.045	0.029
Char Amount (g)	0.2255	0.3021	0.1436	0.1474
Char Yield (%)	38%	51%	18%	28%

Table A3: Gasification run data – Runs 9-12

Run #	9	10	11	12
Sample ID	M04/21/05(2)	M04/25/05(11)	M04/28/05(11)	M04/28/05(111)
Feeding Material	BL	BL	BL	BL
Particle Size (mm)	90 - 125	90 - 125	90 - 125	90 - 125
Residence Time (s)	1.36	1.36	0.876	0.876
Temp. (^{o}C)	1000	1000	1000	1000
N_2 (%)	80	80	80	80
CO_2 (%)	10	10	10	10
Steam (%)	10	10	10	10
Primary flow (ml/min)	124	124	124	124
Seconday flow (L/min)	10	10	10	10
Quench flow (L/min)	10	10	10	10
Feeding Amount (g)	0.6806	0.7822	0.9679	0.8943
Feeding Time (min)	18	20	25	22
Feeding Rate (g/min)	0.038	0.039	0.039	0.041
Char Amount (g)	0.1164	0.1594	0.1668	0.2079
Char Yield (%)	17%	20%	17%	23%

Table A4: Gasification run data – Runs 9-12

Run #	13	14
Sample ID	M05/05/05(11)	M05/05/05(111)
Feeding Material	BL	BL
Particle Size (mm)	90 - 125	90 - 125
Residence Time (s)	0.457	0.457
Temp. (^{o}C)	1000	1000
N_2 (%)	80	80
CO_2 (%)	10	10
Steam (%)	10	10
Primary flow (ml/min)	124	124
Seconday flow (L/min)	10	10
Quench flow (L/min)	10	10
Feeding Amount (g)	0.8463	0.7874
Feeding Time (min)	24	25
Feeding Rate (g/min)	0.035	0.031
Char Amount (g)	0.1335	0.1575
Char Yield (%)	16%	20%

APPENDIX B

DATA ANALYSIS AND CALCULATIONS

Table B1: Order of sampling and corresponding experimental conditions

Sample #	Sample ID	R.T. (s)	Temp. (^{o}C)
<1>	BLS	*	*
<2>	M04/12/05(1)	1.52	900
<3>	M04/13/05(1)	1.52	900
<4>	M04/15/05(1)	0.467	900
<5>	M04/15/05(11)	0.467	900
<6>	M04/19/05(1)	0.906	900
<7>	M04/19/05(11)	0.906	900
<8>	M04/21/05(1)	1.42	900
<9>	M04/21/05(11)	1.42	900
<11>	BL Liquid	*	*
<12>	M04/21/05(2)	1.36	1000
<13>	M04/25/05(11)	1.36	1000
<14>	M04/28/05(11)	0.876	1000
<15>	M04/28/05(111)	0.876	1000
<16>	M05/05/05(11)	0.457	1000
<17>	M05/05/05(111)	0.457	1000

Table B2: Carbonate HS-GC analysis

Sample #	Sample Weight (g)	H_2O Added (mL)	GC File	GC Peak Area	CO_3 (M)	Na_2CO_3 (%)
<1>	0.0291	1	Hou08313.D	51.4	0.03	10.14
<2>	0.0144	1	Hou08314.D	178.7	0.11	78.33
<3>	0.0186	1	Hou08315.D	231.7	0.14	79.44
<4>	0.0144	1	Hou08316.D	168.9	0.10	73.84
<5>	0.0126	1	Hou08317.D	139.0	0.08	68.74
<6>	0.0135	1	Hou08318.D	193.1	0.12	90.59
<7>	0.0163	1	Hou08319.D	222.6	0.13	86.96
<8>	0.0223	1	Hou08320.D	313.6	0.19	90.48
<9>	0.0291	1	Hou08321.D	409.7	0.25	91.12
<11>	0.0257	1	Hou08322.D	41.6	0.02	8.70
<12>	0.0249	1	Hou08324.D	296.9	0.18	76.25
<13>	0.0261	1	Hou08325.D	329.2	0.20	80.83
<14>	0.0191	1	Hou08326.D	255.4	0.15	85.21
<15>	0.0160	1	Hou08327.D	209.8	0.13	83.11
<16>	0.0215	1	Hou08328.D	279.0	0.17	82.87
<17>	0.0151	1	Hou08329.D	208.4	0.12	87.46
		Blank (Standard)	Hou08312.D	6.2		
		0.1 M Na2CO3	Hou08323.D	168.5		

Molarity of Alkali Carbonate Species in Char =

$$0.1 \cdot \frac{A_{sample} - A_{blank}}{A_{0.1M} - A_{blank}}$$

A_{sample} = Peak CO_2 Area of the Char Sample
A_{blank} = Peak CO_2 Area of the Standard (Blank) Solution
$A_{0.1M}$ = Peak CO_2 Area for 0.1M Na_2CO_3

Weight Percent of Alkali Carbonate (Assume all Na_2CO_3) in Char =

$$\frac{M_{CO_3} \cdot 0.00001 \cdot MW_{Na_2CO_3}}{W_{sample}}$$

M_{CO3} = Molarity of Alkali Carbonate Species in the Char
MW_{Na2CO3} = Molecular Weight of Na2CO3 (i.e., 106 g/mol)
W_{sample} = Weight of Char Sample

Table B3: Hydroxide HS-GC analysis

Sample #	Sample ID	GC Peak Area	HCl (M)	Total Acid (M)	OH (M)	NaOH in Char (%)	Na_2CO_3+NaOH in Char (%)
<1>	BLS	151.9	0.15	0.19	0.14	18.73	28.87
<2>	M04/12/05(1)	135.3	0.14	0.23	0.02	4.48	82.81
<3>	M04/13/05(1)	90.1	0.09	0.33	0.05	10.95	90.39
<4>	M04/15/05(1)	156.2	0.16	0.18	-0.02	-5.08	68.76
<5>	M04/15/05(11)	179.1	0.18	0.13	-0.03	-10.19	58.54
<6>	M04/19/05(1)	183.8	0.19	0.12	-0.11	-32.57	58.02
<7>	M04/19/05(11)	134.9	0.14	0.23	-0.04	-9.23	77.73
<8>	M04/21/05(1)	88.4	0.08	0.33	-0.05	-8.47	82.01
<9>	M04/21/05(11)	33.5	0.02	0.46	-0.04	-6.11	85.01
<11>	pre-dried BL	160.8	0.16	0.17	0.13	20.22	28.92
<12>	M04/21/05(2)	41.9	0.03	0.44	0.08	12.68	88.93
<13>	M04/25/05(11)	32.5	0.02	0.46	0.06	9.21	90.03
<14>	M04/28/05(11)	77.4	0.07	0.36	0.05	10.66	95.88
<15>	M04/28/05(111)	99.5	0.10	0.31	0.06	14.46	97.57
<16>	M05/05/05(11)	73.2	0.07	0.37	0.03	5.80	88.67
<17>	M05/05/05(111)	118.4	0.12	0.27	0.02	4.62	92.08
	Blank (Standard)	13.7	0				
	0.1 M Na2CO3	238	0.25				

Molarity of HCl in the Char =

$$0.25 \cdot \frac{A_{sample} - A_{blank}}{A_{0.1M} - A_{blank}}$$

A_{sample} = Peak CO_2 Area of the Char Sample
A_{blank} = Peak CO_2 Area of the Standard (Blank) Solution
$A_{0.1M}$ = Peak CO_2 Area for a Standard NaOH Solution

Total Alkali Species Molarity =

$$0.50 - 2 \cdot M_{HCl}$$

M_{HCl} = Molarity of HCl in the Char

Molarity of Alkali OH (Assume all NaOH) in Char =

$$TA - 2 \cdot M_{CO3}$$

TA = Total Alkali Species Molarity
M_{CO3} = Molarity of Alkali Carbonate Species in the Char

Weight Percent of Alkali OH (Assume all NaOH) in Char =

$$\frac{M_{OH} \cdot 0.0004}{TA}$$

M_{OH} = Molarity of Alkali OH in the Char
TA = Total Alkali Species Molarity

Table B4: Combined alkali, total carbon, and ionic species analysis - BLS

black liquor (oven dried), Na_2CO_3 (wt%)	10.14
black liquor (oven dried), Fixed C (wt%)	35.53
black liquor (oven dried), NaOH (wt%)	18.73
black liquor (oven dried), Total C (wt%)	34.68
black liquor (oven dried), Na (mg/kg)	173000.00
black liquor (oven dried), Na (mol/g)	0.00752
black liquor (oven dried), K (mg/kg)	13100.00
black liquor (oven dried), K (mol/g)	0.00034
black liquor (oven dried), S (mg/kg)	42900.00
black liquor (oven dried), S (mol/g)	0.00134
black liquor (oven dried), Ca (mg/kg)	1020.00

Table B5: Combined alkali, total carbon, and ionic species analysis – runs 1-4

Run #	1	2	3	4
Residence Time (s)	1.52	1.52	0.467	0.467
Temp. (^oC)	900	900	900	900
Char GC Na_2CO_3 (wt%)	78.33	79.44	73.84	68.74
Char Na_2CO_3 as C (wt %)	8.87	8.99	8.36	7.78
Fixed C in Char (wt%)	2.36	1.25	14.96	15.04
Char GC NaOH (wt%)	4.48	10.95	Trace	Trace
Char Total C (wt%)	11.23	10.24	23.32	22.82
Na (mg/kg)	254000.00	331000.00	202000	193000.00
K (mg/kg)	17500	22100	15100	14500
S (mg/kg)	7080	16000	15000	15900
Ca (mg/kg)	1420	2110	1190	1420

Table B6: Combined alkali, total carbon, and ionic species analysis – runs 5-8

Run #	5	6	7	8
Residence Time (s)	0.906	0.906	1.42	1.42
Temp. (^{o}C)	900	900	900	900
Char GC Na_2CO_3 (wt%)	90.59	86.96	90.48	91.12
Char Na_2CO_3 as C (wt %)	10.26	9.84	10.24	10.32
Fixed C in Char (wt%)	6.56	7.48	1.06	1.56
Char GC NaOH (wt%)	Trace	Trace	Trace	Trace
Char Total C (wt%)	16.82	17.32	11.30	11.88
Na (mg/kg)	230000.00	228000.00	294000.00	313000.00
K (mg/kg)	16800	16400	20200	20800
S (mg/kg)	7910	8040	12000	13700
Ca (mg/kg)	1370	1330	1780	1890

Table B7: Combined alkali, total carbon, and ionic species analysis – runs 9-12

Run #	9	10	11	12
Residence Time (s)	1.36	1.36	0.876	0.876
Temp. (^{o}C)	1000	1000	1000	1000
Char GC Na_2CO_3 (wt%)	76.25	80.83	85.21	83.11
Char Na_2CO_3 as C (wt %)	8.63	9.15	9.65	9.41
Fixed C in Char (wt%)	2.07	0.46	0.24	0.24
Char GC NaOH (wt%)	12.68	9.21	10.66	14.46
Char Total C (wt%)	10.70	9.61	9.89	9.65
Na (mg/kg)	348000.00	356000.00	355000.00	352000.00
K (mg/kg)	21500	20900	22500	22500
S (mg/kg)	25000	30000	24200	29500
Ca (mg/kg)	2510	2500	2360	2390

Table B8: Combined alkali, total carbon, and ionic species analysis – runs 13-14

Run #	13	14
Residence Time (s)	0.457	0.457
Temp. (^{o}C)	1000	1000
Char GC Na_2CO_3 (wt%)	82.87	87.46
Char Na_2CO_3 as C (wt %)	9.38	9.90
Fixed C in Char (wt%)	1.46	0.73
Char GC NaOH (wt%)	5.80	4.62
Char Total C (wt%)	10.84	10.63
Na (mg/kg)	308000.00	311000.00
K (mg/kg)	21100	21100
S (mg/kg)	14500	15600
Ca (mg/kg)	1970	2090

Table B9: Alkali species data reliability check – runs 1-4

Run #	1	2	3	4
Residence Time (s)	1.52	1.52	0.467	0.467
Temp. (^{o}C)	900	900	900	900
Na_2CO_3 (mol/g) Char Basis	0.0074	0.0075	0.0070	0.0065
NaOH (mol/g) Char Basis	0.0011	0.0027	Trace	Trace
S (mol/g) Char Basis	0.0002	0.0005	0.0005	0.0005
Na Char Sum	0.0163	0.0187	0.0149	0.0140
Na+K (mol/g) Char Basis	0.0115	0.0150	0.0092	0.0088
% Difference	-42.13	-25.13	-62.09	-59.27

Table B10: Alkali species data reliability check – runs 5-8

Run #	5	6	7	8
Residence Time (s)	0.906	0.906	1.42	1.42
Temp. (^{o}C)	900	900	900	900
Na_2CO_3 (mol/g) Char Basis	0.0085	0.0082	0.0085	0.0086
NaOH (mol/g) Char Basis	Trace	Trace	Trace	Trace
S (mol/g) Char Basis	0.0002	0.0003	0.0004	0.0004
Na Char Sum	0.0176	0.0169	0.0178	0.0180
Na+K (mol/g) Char Basis	0.0104	0.0103	0.0133	0.0141
% Difference	-68.53	-63.58	-33.94	-27.57

Table B11: Alkali species data reliability check – runs 9-12

Run #	9	10	11	12
Residence Time (s)	1.360	1.360	0.876	0.876
Temp. (^{o}C)	1000	1000	1000	1000
Na_2CO_3 (mol/g) Char Basis	0.0072	0.0076	0.0080	0.0078
NaOH (mol/g) Char Basis	0.0032	0.0023	0.0027	0.0036
S (mol/g) Char Basis	0.0008	0.0009	0.0008	0.0009
Na Char Sum	0.0191	0.0194	0.0203	0.0211
Na+K (mol/g) Char Basis	0.0157	0.0160	0.0160	0.0159
% Difference	-21.66	-21.26	-26.46	-33.06

Table B12: Alkali species data reliability check – runs 13-14

Run #	13	14
Residence Time (s)	0.457	0.457
Temp. (^{o}C)	1000	1000
Na_2CO_3 (mol/g) Char Basis	0.0078	0.0083
NaOH (mol/g) Char Basis	0.0015	0.0012
S (mol/g) Char Basis	0.0005	0.0005
Na Char Sum	0.0180	0.0186
Na+K (mol/g) Char Basis	0.0139	0.0141
% Difference	-29.09	-32.43

Table B13: Calculated data – runs 1-4

Run #	1	2	3	4
Residence Time (s)	1.52	1.52	0.467	0.467
Temp. (^{o}C)	900	900	900	900
Char Yield (Ca Method)	0.718	0.483	0.857	0.718
Char Yield (%)	72	48	86	72
Avg. Char Yield (%)	60	**	79	**
Std. Dev. Char Yield (%)	17	**	10	**
Na in Char (mol/g Char)	0.0110	0.0144	0.0088	0.0084
K in Char (mol/g Char)	0.0004	0.0006	0.0004	0.0004
S in Char (mol/g Char)	0.0002	0.0005	0.0005	0.0005
Total C in Char (mol/g Char)	0.0094	0.0085	0.0194	0.0190
Fixed C in Char (mol/g Char)	0.0020	0.0010	0.0125	0.0125
Na+K in Char (mol/g Char)	0.0115	0.0150	0.0092	0.0088
Amount of Na in Char Alkali (%)	96.10	96.21	95.78	95.76
Amount of K in Char Alkali (%)	3.90	3.79	4.22	4.24
Na_2CO_3 in Char (mol/g Char)	0.0074	0.0075	0.0070	0.0065
Na_2CO_3 in Char (mol/g BLS fed)	0.0053	0.0036	0.0060	0.0047
NaOH in Char (mol/g Char)	0.0011	0.0027	Trace	Trace
NaOH in Char (mol/g BLS fed)	0.0008	0.0013	Trace	Trace
NaOH/(NaOH +2*Na_2CO_3) (mol%)	7%	15%	Trace	Trace
Fraction of Na Retained in Char	105%	92%	100%	80%
Fraction of K Retained in Char	96%	82%	99%	80%
Fraction of S Retained in Char	12%	18%	30%	27%
Fraction of C Retained in Char	23%	14%	58%	47%
Fixed C Retained in Char	5.1%	1.8%	38%	32%
Total C in Char (%C Input in BLS)	23%	14%	58%	47%
Fixed C in Char (%C Input in BLS)	5.1%	1.8%	38%	32%
Carbonate C in Char (%C Input in BLS)	18%	13%	21%	16%

Table B14: Calculated data – runs 5-8

Run #	5	6	7	8
Residence Time (s)	0.906	0.906	1.42	1.42
Temp. (^{o}C)	900	900	900	900
Char Yield (Ca Method)	0.745	0.767	0.573	0.540
Char Yield (%)	74	77	57	54
Avg. Char Yield (%)	76	**	56	**
Std. Dev. Char Yield (%)	2	**	2	**
Na in Char (mol/g Char)	0.0100	0.0099	0.0128	0.0136
K in Char (mol/g Char)	0.0004	0.0004	0.0005	0.0005
S in Char (mol/g Char)	0.0002	0.0003	0.0004	0.0004
Total C in Char (mol/g Char)	0.0140	0.0144	0.0094	0.0099
Fixed C in Char (mol/g Char)	0.0055	0.0062	0.0009	0.0013
Na+K in Char (mol/g Char)	0.0104	0.0103	0.0133	0.0141
Amount of Na in Char Alkali (%)	95.87	95.93	96.11	96.23
Amount of K in Char Alkali (%)	4.13	4.07	3.89	3.77
Na_2CO_3 in Char (mol/g Char)	0.0085	0.0082	0.0085	0.0086
Na_2CO_3 in Char (mol/g BLS fed)	0.0064	0.0063	0.0049	0.0046
NaOH in Char (mol/g Char)	Trace	Trace	Trace	Trace
NaOH in Char (mol/g BLS fed)	Trace	Trace	Trace	Trace
NaOH/(NaOH +2*Na_2CO_3) (mol%)	Trace	Trace	Trace	Trace
Fraction of Na Retained in Char	99%	101%	97%	98%
Fraction of K Retained in Char	95%	96%	88%	86%
Fraction of S Retained in Char	14%	14%	16%	17%
Fraction of C Retained in Char	36%	38%	19%	18%
Fixed C Retained in Char	15%	17%	1.8%	2.5%
Total C in Char (%C Input in BLS)	36%	38%	19%	18%
Fixed C in Char (%C Input in BLS)	15%	17%	1.8%	2.5%
Carbonate C in Char (%C Input in BLS)	22%	22%	17%	16%

Table B15: Calculated data – runs 9-14

Run #	9	10	11	12	13	14
Residence Time (s)	1.36	1.36	0.876	0.876	0.457	0.457
Temp. (^{o}C)	1000	1000	1000	1000	1000	1000
Char Yield (Ca Method)	0.406	0.408	0.432	0.427	0.518	0.488
Char Yield (%)	41	41	43	43	52	49
Avg. Char Yield (%)	41	**	43	**	50	**
Std. Dev. Char Yield (%)	0	**	0	**	2	**
Na in Char (mol/g Char)	0.0151	0.0155	0.0154	0.0153	0.0134	0.0135
K in Char (mol/g Char)	0.0005	0.0005	0.0006	0.0006	0.0005	0.0005
S in Char (mol/g Char)	0.0008	0.0009	0.0008	0.0009	0.0005	0.0005
Total C in Char (mol/g Char)	0.0089	0.0080	0.0082	0.0080	0.0090	0.0089
Fixed C in Char (mol/g Char)	0.0017	0.0004	0.0002	0.0002	0.0012	0.0006
Na+K in Char (mol/g Char)	0.0157	0.0160	0.0160	0.0159	0.0139	0.0141
Amount of Na in Char Alkali (%)	96.58	96.66	96.40	96.37	96.12	96.15
Amount of K in Char Alkali (%)	3.42	3.34	3.60	3.63	3.88	3.85
Na_2CO_3 in Char (mol/g Char)	0.0072	0.0076	0.0080	0.0078	0.0078	0.0083
Na_2CO_3 in Char (mol/g BLS fed)	0.0029	0.0031	0.0035	0.0033	0.0040	0.0017
NaOH in Char (mol/g Char)	0.0032	0.0023	0.0027	0.0036	0.0015	0.0012
NaOH in Char (mol/g BLS fed)	0.0013	0.0005	0.0005	0.0008	0.0002	0.0002
NaOH/(NaOH +2*Na_2CO_3) (mol%)	18%	13%	14%	19%	8%	7%
Fraction of Na Retained in Char	82%	84%	89%	87%	92%	88%
Fraction of K Retained in Char	65%	65%	74%	73%	83%	79%
Fraction of S Retained in Char	23%	29%	24%	29%	18%	18%
Fraction of C Retained in Char	13%	11%	12%	12%	16%	15%
Fixed C Retained in Char	3%	0.6%	0.3%	0.3%	2.3%	1.1%
Total C in Char (%C Input in BLS)	13%	11%	12%	12%	16%	15%
Fixed C in Char (%C Input in BLS)	2.5%	0.6%	0.3%	0.3%	2.3%	1.1%
Carbonate C in Char (%C Input in BLS)	10%	11%	12%	12%	14%	14%

APPENDIX C

SAMPLE CALCULATIONS

Table C1: Summary of analysis results for gasification at 900°C, 1.52 s residence Time

Residence Time (s)	1.52
Temp. (°C)	900
Char GC Na_2CO_3 (wt%)	78.33
Char GC NaOH (wt%)	4.48
Char Total C (wt%)	11.23
Na (mg/kg)	254000.00
K (mg/kg)	17500
S (mg/kg)	7080
Ca (mg/kg)	1420

Determination of Carbonate Carbon (i.e., C Tied to Na_2CO_3 in the Char):

$$\text{Carbonate Carbon in Char (wt\%)} = \frac{MW_C}{MW_{Na_2CO_3}} \cdot X_{Na_2CO_3}$$

MW_C = Atomic Mass of C (12 g/mol)
MW_{Na2CO3} = Molecular Weight of Na_2CO_3 (106 g/mol)
X_{Na2CO3} = Weight Percent of Na_2CO_3 in Char from GC Measurement

If X_{Na2CO3} = 78.33%,
Carbonate Carbon in Char = 6/53*78.33 = 8.87%

The Carbonate Carbon in BLS is determined in the same manner.

Fixed Carbon in Char:

Fixed Carbon = Total Carbon – Carbonate Carbon in Char

If Total Carbon (wt%) = 11.23%
If Carbonate Carbon in Char (wt%) = 8.87%
Fixed Carbon in Char = 11.23 – 8.87 = 2.36%

The Fixed Carbon in BLS is determined in the same manner.

Char Residue Yield Determination:

Char Yield = Mass of Char Residue/Mass of BLS = X_{Ca_BLS}/X_{Ca_Char}

X_{Ca_BLS} = Concentration of Calcium in BLS (mg/kg)
X_{Ca_Char} = Concentration of Calcium in Char (mg/kg)

If X_{Ca_BLS} = 1020 mg/kg and X_{Ca_Char} = 1420 mg/kg,

Char Yield = 1020/1420 = 0.718 => 72%

Calculations for Na and K in the Char:

$$\text{Na in Char (mol/g Char)} = \frac{X_{Na}}{1000000 \cdot 23}$$

$$\text{K in Char (mol/g Char)} = \frac{X_{K}}{1000000 \cdot 39}$$

X_{Na} = Concentration of Na in Char (mg/kg)
X_K = Concentration of K in Char (mg/kg)

Na + K in Char = $X_{Na} + X_K$

If X_{Na} = 254000 mg/kg and X_K = 17500 mg/kg,

Na in Char = 254000/100000/23 = 0.0110 mol/g Char
K in Char = 17500/100000/39 = 0.0004 mol/g Char
Na + K in Char = 0.0110 + 0.0004 = 0.0115 mol/g Char

Percentage of Na in Char = Na in Char/(Na + K in Char),

Percentage of Na in Char = 0.0110/0.115 = 0.961 => 96.1% Na

Hydroxide Formation Calculations:

$$Na_2CO_3 \text{ in Char (mol/g Char)} = \frac{X_{Na_2CO_3}}{100 \cdot MW_{Na_2CO_3}}$$

MW_{Na2CO3} = Molecular Weight of Na_2CO_3 (106 g/mol)
X_{Na2CO3} = Weight Percent of Na_2CO_3 in Char from GC Measurement

If X_{Na2CO3} = 78.33%,
Na_2CO_3 in Char (mol/g Char) = 78.33/100/106 = 0.0074 mol/g Char

$$\text{NaOH in Char (mol/g Char)} = \frac{X_{NaOH}}{100 \cdot MW_{Na_2OH}}$$

X_{NaOH} = Weight Percent of NaOH in Char from GC Measurement
MW_{NaOH} = Molecular Weight of NaOH (40 g/mol)

If X_{NaOH} = 4.48%
NaOH in Char (mol/g Char) = 4.48/100/40 = 0.0011 mol/g Char

$$\text{NaOH in Char from All Alkali Species} = \frac{X'_{NaOH}}{X'_{NaOH} + 2 \cdot X'_{Na_2CO_3}}$$

X'_{NaOH} = NaOH in Char (mol/g Char)
X'_{Na2CO3} = Na_2CO_3 in Char (mol/g Char)

If X'_{NaOH} = 0.0011 mol/g Char and X'_{Na2CO3} = 0.0074 mol/g Char,
NaOH in Char from All Alkali Species = 0.0011/(0.0011 + 2*0.0074) = 7%

Na and K Retention in Char:

$$\text{Fraction of Na Retained in Char} = \frac{CY \cdot X_{Na}}{X_{Na\_BLS}}$$

CY = Char Yield
X_{Na} = Concentration of Na in Char (mg/kg)
X_{Na_BLS} = Concentration of Na in BLS (mg/kg)

If X_{Na} = 254000 mg/kg and X_{Na_BLS} = 173000 mg/kg
And if CY = 72%,
Fraction of Na Retained in Char = 0.72*254000/173000 = 1.05 => 105%

$$\text{Fraction of K Retained in Char} = \frac{CY \cdot X_{K}}{X_{K\_BLS}}$$

CY = Char Yield
X_K = Concentration of K in Char (mg/kg)
X_{K_BLS} = Concentration of K in BLS (mg/kg)

If X_K = 17500 mg/kg and X_{K_BLS} = 13100 mg/kg
And if CY = 72%,

Fraction of K Retained in Char = 0.72*17500/13100 = 0.96 => 96%

Carbon in Terms of C Input in BLS:

$$\text{Total C in Char (\%C Input in BLS)} = \frac{X_{Total\_C} \cdot CY}{X_{Total\_C\_BLS}}$$

CY = Char Yield
X_{Total_C} = Total Carbon in Char (wt%)
$X_{Total\_C\_BLS}$ = Total Carbon in BLS (wt%)

If X_{Total_C} = 11.23% and $X_{Total\_C\_BLS}$ = 34.68%
And if CY = 72%,

Total C in Char (%C Input in BLS) = 11.23*0.72/34.68 = 0.23 => 23%

$$\text{Fixed C in Char (\%C Input in BLS)} = \frac{X_{Fixed\_C} \cdot CY}{X_{Total\_C\_BLS}}$$

$$\text{Fixed C in BLS (\%C Input in BLS)} = \frac{X_{Fixed\_C\_BLS}}{X_{Total\_C\_BLS}}$$

CY = Char Yield
X_{Fixed_C} = Fixed Carbon in Char (wt%)
$X_{Total\_C\_BLS}$ = Total Carbon in BLS (wt%)
$X_{Fixed\_C\_BLS}$ = Fixed Carbon in BLS (wt%)

If X_{Fixed_C} = 2.36%, $X_{Fixed\_C\_BLS}$ = 33.53%, and $X_{Total\_C\_BLS}$ = 34.68%
And if CY = 72%,

Fixed C in Char (%C Input in BLS) = 2.36*0.72/34.68 = 0.049 => 4.9%
Fixed C in BLS (%C Input in BLS) = 33.53/34.68 = 0.967 => 96.7%

$$\text{Carbonate C in Char (\%C Input in BLS)} = \frac{X_{Carbonate\_C} \cdot CY}{X_{Total\_C\_BLS}}$$

$$\text{Carbonate C in BLS (\%C Input in BLS)} = \frac{X_{Carbonate\_C\_BLS}}{X_{Total\_C\_BLS}}$$

CY = Char Yield
$X_{Carbonate\_C\_BLS}$ = Carbonate Carbon in BLS (wt%)
$X_{Carbonate\_C}$ = Carbonate Carbon in Char (wt%)
$X_{Total\_C\_BLS}$ = Total Carbon in BLS (wt%)

If $X_{Carbonate\_C}$ = 8.87%, $X_{Carbonate\_C\_BLS}$ = 1.15%, and $X_{Total\_C\_BLS}$ = 34.68%
And if CY = 72%,

Carbonate C in Char (%C Input in BLS) = 8.87*0.72/34.68 = 0.18 => 18%
Carbonate C in BLS (%C Input in BLS) = 1.15/34.68 = 0.033 => 3.3%

APPENDIX D

SUMMARY OF LEFR SIMULATIONS

Table D1: Input parameters for the LEFR simulations

Secondary Gas Flow (lpm)	10
Primary Gas Flow (lpm)	0.12
Secondary Inlet Temp (K)	1273
Primary Inlet Temp (K)	300
Glow Bar Temp (K)	1273
Injector Diameter (mm ID)	3.3
H_2O gas %	10
CO_2 gas %	10
N_2 gas %	80
Particle Density (kg/m^3)	73
Initial Particle Diameter (microns)	90
Max Particle Diameter (microns)	270
Kinetic Rate Model	Li and van Heinigen
Weight % Solid in Particle	100
C (%)	35.6
H (%)	3.34
Na (%)	18.8
O (%)	36.6
S (%)	4.06
other (%)	1.6
Sulfur Species Composition in Solid	
Sulfide	0.13
Sulfate	4.53
Thiosulfate	0
Sulfite	0
Organic Sulfur	0.74
Black Liquor Feed Rate (g/s)	0.0017
Fraction Na Volatilized after Pyrolysis	0.08
C/Na in Char after Pyrolysis	3.12
% Sulfite Conversion in Gasification	100
Black Liquor Type	Pine
Heat Capacity Constant (J/kg/K)	4309

Table D2: Temperature-dependent heat capacity parameters

first constant (1073.95 K)	
A	57.264
B	-15.484
C	-3.782
D	23.527
second constant (1373.15 K)	
A	77.7638
B	-7.5312
C	0
D	0

Table D3: Simulation output – residence time versus particle heating zone length

R.T. (s)	X (m)	X (cm)	Y (cm)	Y (in)
0.1	0.0886	8.86	3.16	1.264
0.15	0.131	13.1	7.4	2.96
0.2	0.174	17.4	11.7	4.68
0.25	0.216	21.6	15.9	6.36
0.3	0.258	25.8	20.1	8.04
0.35	0.299	29.9	24.2	9.68
0.4	0.34	34	28.3	11.32
0.45	0.381	38.1	32.4	12.96
0.5	0.422	42.2	36.5	14.6
0.55	0.463	46.3	40.6	16.24
0.6	0.503	50.3	44.6	17.84
0.65	0.543	54.3	48.6	19.44
0.7	0.584	58.4	52.7	21.08
0.75	0.624	62.4	56.7	22.68
0.8	0.664	66.4	60.7	24.28
0.85	0.704	70.4	64.7	25.88
0.9	0.744	74.4	68.7	27.48
0.95	0.784	78.4	72.7	29.08
1	0.823	82.3	76.6	30.64
1.1	0.899	89.9	84.2	33.68
1.2	0.978	97.8	92.1	36.84
1.3	1.05	105	99.3	39.72
1.4	1.122	112.2	106.5	42.6
1.5	1.194	119.4	113.7	45.48
1.6	1.266	126.6	120.9	48.36
1.7	1.338	133.8	128.1	51.24
1.8	1.41	141	135.3	54.12
1.9	1.482	148.2	142.5	57
2	1.554	155.4	149.7	59.88

Notes about Table D3:

BL feed rate = 0.1 g/min
Valid for 973 K and 1073 K furnace temperatures
Valid for both constant and non-constant heat capacities
MW = 57.443 g/mol

X = Length of Heating Zone in LEFR
Y = Actual Particle Travel Distance (i.e., Actual Zone Length) in LEFR

Y (cm) = X (cm) – 5.7

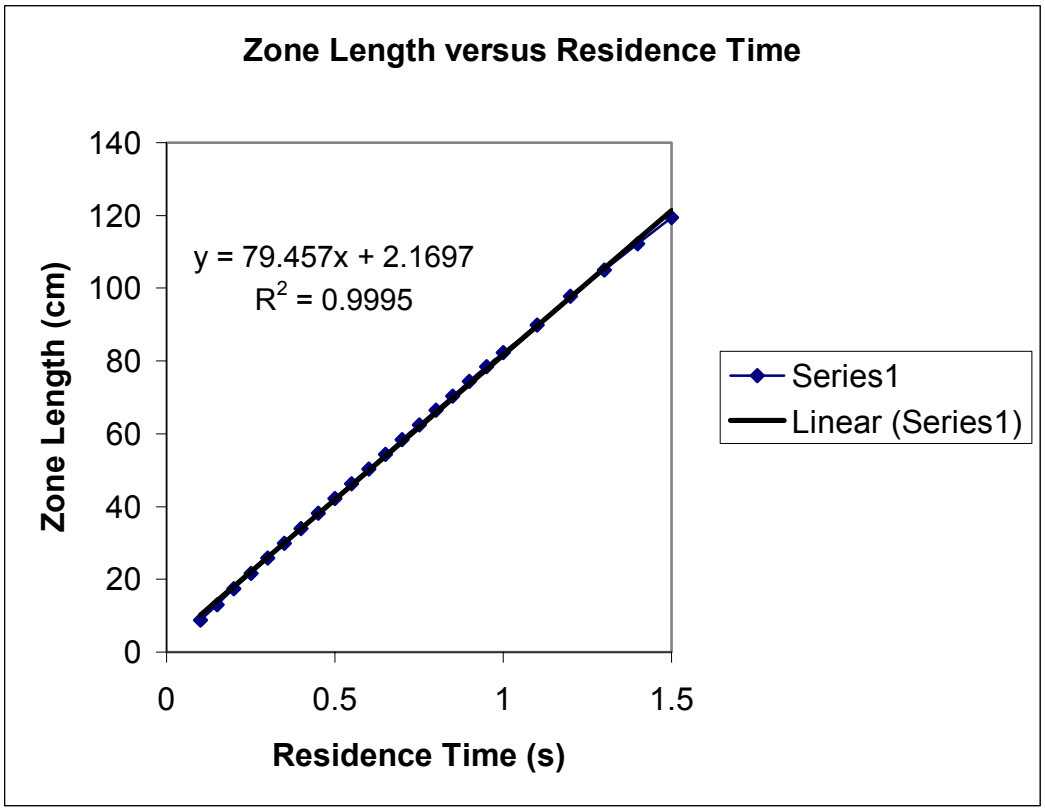

Figure D1: Zone length versus residence time in the LEFR

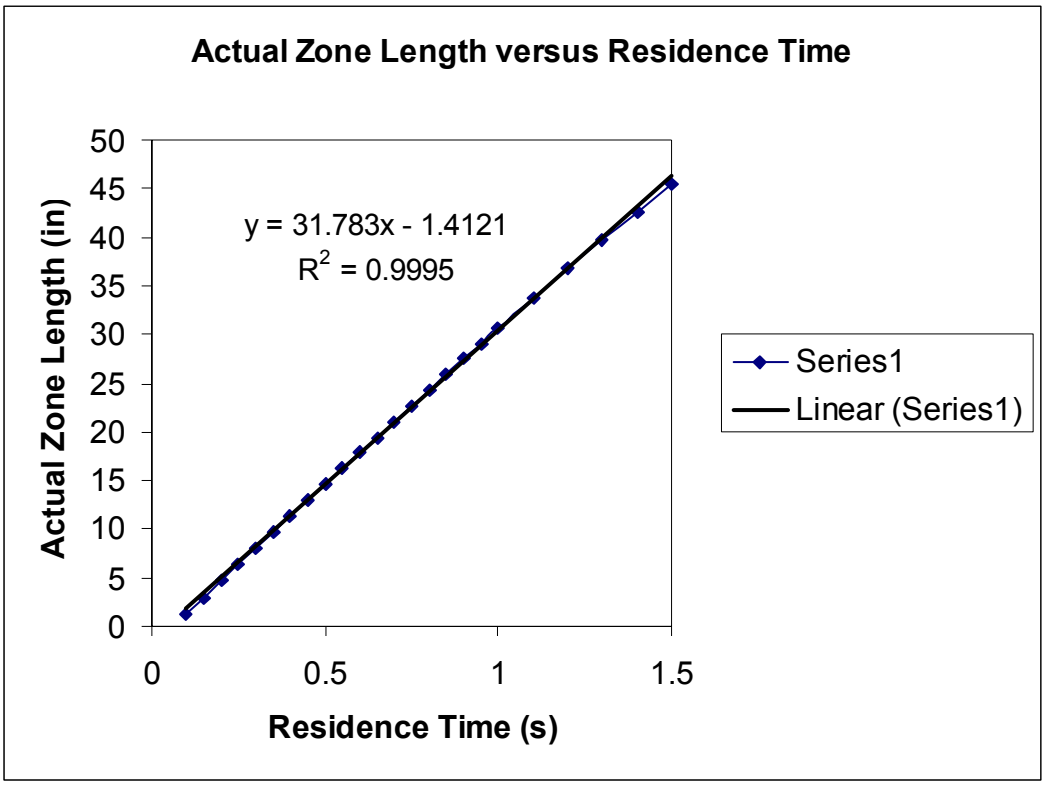

Figure D2: Actual heating zone length versus residence time in the LEFR

BIBLIOGRAPHY

1. "Analysis of Pulping Liquors by Suppressed Ion Chromatography," TAPPI Test Method T 699 om-00, Atlanta (2000).

2. Barrio, M., Gobel, B., Risnes, H., Henriksen, U., Hustad, J.E., and Sorensen, L.H., "Steam Gasification of Wood Char and the Effect of Hydrogen Inhibition on the Chemical Kinetics," Report, Norwegian University of Science and Technology (2004).

3. Barrio, M., "Hydrogen from Biomass Gasification," Ph.D Dissertation, Institute of Thermal Energy and Hydropower, Norwegian University of Science and Technology (2005).

4. Bell, D., "Black Liquor Gasification Offers Increased Yield, Power Generation, and Profit," Press Release, Institute of Paper Science and Technology, April 30, 2003. http://www.ipst.gatech.edu/news/archive/2003/030430black_liquor.html

5. Berglin, N., Stigsson, L., "Black Liquor Gasification – Towards Improved Pulp and Energy Yields," 6th International Conference on New Available Technologies, Stockholm, Sweden (1999).

6. Biermann, C.J., "Handbook of Pulp and Papermaking," 2ed., Academic Press, San Diego, pp. 108 (1996).

7. Blum, L., "The Production of Bleached Kraft Pulp," Environmental Defense Fund, 1996. http://www.rfu.org/KraftPulp.htm

8. Boss, C., Fredeen, K., "Concepts, Instrumentation, and Techniques in Inductively Coupled Plasma Atomic Emission Spectroscopy," Perkin Elmer Instrumentation Guide, New York (1989).

9. Cameron, J.H., Grace, T.M., "Kinetic Study of Sulfate Reduction with Kraft Black Liquor Char," Industrial and Engineering Chemistry Fundamentals, 24(4): 443-449 (1985).

10. Cerfontain, M.B., Meijer, R., Kapteijn, F., and Moulijn, J.A., "Alkali Catalyzed Carbon Gasification in CO/CO_2 Mixtures; an Extended Model for the Oxygen Exchange and Gasification Reaction," Journal of Catalysis, 107: 173-180 (1987).

11. Chai, X.S., Dhasmana, B., and Zhu, J.Y., "Determination of Volatile Organic Compound contents in Kraft Mill Streams Using Headspace Gas Chromatography," Journal of Pulp and Paper Science, 24 (2): 50-54 (1998).

12. Chai, X-S., Luo, Q., and Zhu, J.Y., "Analysis of Nonvolatile Species in a Complex Matrix by Headspace Gas Chromatography," Journal of Chromatography A, 909: 249-257 (2001).

13. Chen, S.G., Yang, R.T., "The Active Surface Species in Alkali-Catalyzed Carbon Gasification: Phenolate (C-O-M) Groups versus Clusters (Particles)," Journal of Catalysis, 141: 102-113 (1993).

14. Chen, S.G., and Yang, R.T., "Unified Mechanism of Alkali and Alkaline Earth Catalyzed Gasification Reactions of Carbon by CO_2 and H_2O," Energy and Fuels, 11: 421-427 (1997).

15. Covey, G.H., "Development of the Direct Alkali Recovery System and Potential Applications," Pulp and Paper Journal of Canada, 83(12): T350-T354 (1982).

16. Covey, G.H., "Development of the Direct Alkali Recovery System and Potential Applications," TAPPI International Conference on Recovery of Pulping Chemicals, Vancouver (1981).

17. Covey, G.H., Frederick, W.J., and Harrison, R.E., "A Study of the Sensitivity of Energy Recovery to Design and Operating Parameters in a DARS Plant," AIChE Symposium Series, 246(81) (1985).

18. Edin, M., "Influence of Carbon Dioxide on the Kinetics of the Reaction between Sodium Carbonate and Sodium Trititanate," MS Thesis, Lulea University of Technology (2000).

19. Eriksson, H., Harvey, S., "Black Liquor Gasification – Consequences for Both Industry and Society," Energy, 29: 581-612 (2004).

20. Evans, R.E., Milne, T., "Molecular Characterization of the Pyrolysis of Biomass. 1. Fundamentals," Energy and Fuels, 1(2) (1987).

21. Farmer, M., Sinquefield, S., "An External Benefits Study of Black Liquor Gasification," Final Report, Georgia Institute of Technology, June 15, 2003.

22. Flaxman, R.J., "Flow and Particle Heating in an Entrained Flow Reactor," MS Thesis, University of Ottawa (1986).

23. Forest Sweden: Pulp and Paper, SkogsSverige, 2005. http://www.skogssverige.se/MassaPapper/Faktaom/eng/massaopapptillv/sulfkemi.cfm

24. "Fossil Fuels: Coal Utilization: Gasification," Extraction and Processing Industries, Britannica Online. http://www.eb.com:180/cgi-bin/g?DocF=macro/5003/11/278.html

25. Frederick, W.J, "Black Liquor Properties," Kraft Recovery Boilers, TAPPI Press, Atlanta, pp. 77 (1997).

26. Frederick, W.J., Hupa, M.M., "Gasification of Black Liquor Char with CO_2 at Elevated Pressures," TAPPI Journal, 74(7): 177-184 (1991).

27. Frederick, W. J., Hupa M., and Uusikartano, T., "Volatiles and Char Carbon Yields during Black Liquor Pyrolysis," Bioresource Technology, 48: 59-64 (1994).

28. Frederick, W.J., Wåg, K.J., and Hupa, M.M., "Rate and Mechanism of Black Liquor Char Gasification with CO_2 at Elevated Pressures," Industrial and Engineering Chemistry Research, 32: 1747-1753 (1993).

29. Gairns, S.A., Kubes, G.J., and van Heinigen, A.R.P., "New Insights into TRS Gas Formation during Pyrolysis of Black Liquor," AIChE Spring National Meeting, Atlanta, 104d (1994).

30. Grace, T.M., "Chemical Recovery Process Chemistry," Chemical Recovery in the Alkaline Pulping Process 3ed, pp. 57-78, Atlanta: TAPPI Press, 1992.

31. Horenziak, S., "Examination of Sulfurous Products from the Gasification of Kraft Black Liquor Solids," A190 Independent Research Final Report, Institute of Paper Science and Technology (1999).

32. Hupa, M., Solin, P., and Hyöty, P., "Combustion Behavior of Black Liquor Droplets," Journal of Pulp and Paper Science, 13(2): J67-72 (1987).

33. Iisa, K., Sinquefield, S.A., and Jing, K., "Gasification of Black Liquor," Summary Report for Project F028, Institute of Paper Science and Technology (1999).

34. Jarvinen, M., "Black Liquor Recovery Boilers," Lecture Slides, ENE 47-132 Combustion and Gasification Technology, Helsinki University of Technology (2004).

35. Jarvinen, M., Zevenhoven, R., Vakkilainen, E., and Forssen, M., "Black Liquor Devolatilization and Swelling – a Detailed Droplet Model and Experimental Validation," Biomass and Bioenergy, 24: 495-509 (2003).

36. Jivakanun, N., "Reaction Kinetics for Black Liquor Pyrolysis and Gasification - Plug Series," MS Thesis, Oregon State University (1993).

37. Larsen, E., Consonni, S., Katofsky, R., "A Cost-Benefit Assessment of Biomass Gasification Power Generation in the Pulp and Paper Industry," Final Report, Princeton Environmental Institute, October 8, 2003.

38. Larsen, E., Kreutz, T., Consonni, S., "Performance and Preliminary Economics of Black Liquor Gasification Combined Cycles for a Range of Kraft Pulp Mill Sizes," TAPPI International Chemical Recovery Conference, Tampa, FL (1998).

39. Larsen, E., McDonald, G., Yang, W., Frederick, W., Iisa, K., Kreutz, T., Malcolm, E., and Brown, C., "A Cost-Benefit Assessment of BLGCC Technology," TAPPI Journal, 83(6): 1-15 (2000).

40. Larson, E.D., Yang, W., Iisa, K., Malcolm, E.W., McDonald, G.W., Frederick, W.J., Kreutz, T.G., and Brown, C.A., "A Cost-Benefit Assessment of Black Liquor Gasifier/Combined Cycle Technology Integrated into a Kraft Pulp Mill," Proceedings of the International Chemical Recovery Conference, 1: 1-18 (1998).

41. Li, J., and Van Heinigen, A.R.P., "Kinetics of CO_2 Gasification of Fast Pyrolysis Black Liquor Char," Industrial and Engineering Chemistry Research, 29(9): 1776-1785 (1990).

42. Li, J., and Van Heinigen, A.R.P., "Kinetics of Gasification of Black Liquor Char by Steam," Industrial and Engineering Chemistry Research, 30(7): 1594-1601 (1991).

43. Li, J., and Van Heinigen, A.R.P., "Sodium Emission During Pyrolysis and Gasification of Black Liquor Char," TAPPI Journal, 73(12): 213-219 (1990).

44. Li, J., van Heiningen, A.R.P., "Sulfur Emission During Slow Pyrolysis of Kraft Black Liquor," TAPPI Journal, 74(3): 237-239 (1991).

45. Littau, M., Wåg, K.J., Frederick, W.J., and Jivakanun, N., "Modification and Testing of an Entrained-Flow Black Liquor Gasifier FORTRAN Model," Department of Chemical Engineering Report, Oregon State University, December 19, 1994.

46. Marklund, M., "Numerical Modeling of the CHEMREC Black Liquor Gasification Process," MS Thesis, Lulea University of Technology (2001).

47. Martin, N., Anglani, N., Einstein, D., Khrushch, M., Worrell, E., and Price, L.K., "Opportunities to Improve Energy Efficiency and Reduce Greenhouse Gas Emissions in the U.S. Pulp and Paper Industry," Report, Ernest O. Lawrence Berkeley National Laboratory, July 2000.

48. Mims, C.A., Pabst, J.K., "Alkali-Catalyzed Carbon Gasification Kinetics: Unification of H_2O, D_2O, and CO_2 Reactivities," Journal of Catalysis, 107: 209-220 (1987).

49. Mims, C.A., Pabst, J.K., Melchior, M.T., and Rose, K.D., "Characterization of Catalyzed Carbon Surfaces by Derivatization and Solid-State NMR," Journal of the American Chemical Society, 104: 6886-6887 (1982).

50. Nilsson ,L.J., Larson E.D., Gilbreath K.R., and Gupta A, "Energy Efficiency and the Pulp and Paper Industry," ACEEE, Washington DC/Berkeley CA (1995).

51. Nohlgren, I., "Non-conventional Causticization Technology: A Review," Nordic Pulp and Paper Research Journal, 19(4): 467-477 (2004).

52. Nohlgren, I., "Recovery of Kraft Black Liquor with Direct Causticization using Titanates," Ph.D Disseration, Lulea University of Technology (2002).

53. Nohlgren, I., Sinquefield, S., "Black Liquor Gasification with Direct Causticization using Titanates: Equilibrium Calculations," Industrial and Engineering Chemistry Research, 43: 5996-6000 (2004).

54. Nohlgren, I., Sricharoenchaikul, V., Sinquefield, S., Frederick, W.J., and Theilander, H., "Black Liquor Gasification with Direct Causticization using Titanates in a Pressurized Entrained-Flow Reactor, Part 1: Kinetics of the Causticization Reaction," Journal of Pulp and Paper Science, 29(4): 107-113 (2003).

55. Nohlgren, I., Sricharoenchaikul, V., Sinquefield, S., Frederick, W.J., and Theilander, H., "Black Liquor Gasification with Direct Causticization using Titanates in a Pressurized Entrained-Flow Reactor, Part 2: Carbon Species Transitions," Journal of Pulp and Paper Science, 29(10): 348-355 (2003).

56. Phimolmas, V., "The Effect of Temperature and Residence Time on the Distribution of Carbon, Sulfur, and Nitrogen between Gaseous and Condensed Phase Products from Low Temperature Pyrolysis of Kraft Black Liquor," MS Thesis, Oregon State University (1997).

57. Reeve, D.W. "Kraft Recovery Boilers," Kraft Recovery Operations Short Course, 1992. 1-16.

58. Reis, V. V., Frederick, W. J., Wåg, K. J., Iisa, K., and Sinquefield, S. A., "The Effects of Temperature and Oxygen Concentration on Potassium and Chloride Enrichment during Black Liquor Combustion," TAPPI Journal, 78(12): 67-76 (1995).

59. Settle, F., "Handbook of Instrumental Techniques for Analytical Chemistry," Prentice-Hall, Inc., Princeton, pp. 257 (1997).

60. Sinquefield, S., Nohlgren, I., Ball, A., and Zeng, X., "Direct Causticization for Low and High Temperature Black Liquor Gasification," TAPPI International Chemical Recovery Conference, Charleston, SC (2004).

61. Sprouse, K.M., Schuman, M.D., "Predicting Lignite Devolatilization with the Multiple Parallel and Two-Competing Reaction Models;" Combustion Flame, 43: 265-271 (1981).

62. Sricharoenchaikul, V., "Fate of Carbon-Containing Compounds from Gasification of Kraft Black Liquor with Subsequent Catalytic Conditioning of Condensable Organics," Ph.D Dissertation, Georgia Institute of Technology (2001).

63. Sricharoenchaikul, V., Frederick, W.J., Iisa, K., and Sinquefield, S., "The Role and Fate of Alkali Metals in Black Liquor Combustion," Conference of the Suomen

Soodakattilayhdistys – Finnish Recovery Boiler Conference, Poorvoo, Finland (2004).

64. Sricharoenchaikul, V., Frederick, W.J., and Agrawal, P., "Black Liquor Gasification Characteristics. 1. Formation and Conversion of Carbon-Containing Product Gases," Industrial and Engineering Chemistry Research, 41: 5640-5649 (2002).

65. Sricharoenchaikul, V., Frederick, W.J., and Agrawal, P., "Black Liquor Gasification Characteristics. 2. Measurement of Condensable Organic Matter (Tar) at Rapid Heating Conditions," Industrial and Engineering Chemistry Research, 41: 5650-5658 (2002).

66. Sricharoenchaikul, V., Frederick, W.J., and Agrawal, P, "Carbon Distribution in Char Residue from Gasification of Kraft Black Liquor," Biomass and Bioenergy, 25: 209-220 (2003).

67. Sricharoenchaikul, V, Hicks, A.L, and Frederick, W.J., "Carbon and Char Residue Yields from Rapid Pyrolysis of Kraft Black Liquor," Bioresource Technology, 77(2): 131-138 (2001).

68. Sricharoenchaikul, V., Phimolmas, V., Frederick, W., and Grace, T., "Pyrolysis of Kraft Black Liquor: Formation and Thermal Conversion of Volatile Products and Char," Journal of Pulp and Paper Science, 24(2): J43-50 (1998).

69. Sricharoenchaikul, V., "Sulfur Species Transformation and Sulfate Reduction during Pyrolysis of Kraft Black Liquor," MS Thesis, Oregon State University (1995).

70. Sullivan, J., Douek, M., "Analysis of Hydroxide, Inorganic Sulfur Species, and Organic Anions in Kraft Pulping Liquors by Capillary Electrophoresis," Journal of Chromatography A., 1039: 215-225 (2004).

71. Verrill, C.L. and Wessel, R.A., "Sodium Loss During Black Liquor Drying and Devolatilization- Application of Modeling Results to Understanding Laboratory Data". Proceedings of the International Chemical Recovery Conference, Toronto: B89-B103 (1995).

72. Wåg, K.J., Frederick, W.J., Dayton D.C., and Kelley, S.S., "Characterization of Black Liquor Char Gasification Using Thermogravimetry and Molecular Beam Mass Spectrometry," AIChE Symposium Series, 93(315): 67-76 (1997).

73. Zeng, L., "Kraft Black Liquor Gasification and Direct Causticization in a Fluidized Bed," Ph.D Dissertation, University of New Brunswick (1997).